Thesis for the Degree of Master of Science

Protein tyrosine phosphatase 1B and α-glucosidase inhibitory activities of *Pueraria lobata* roots and its constituents

by

Su Hui Seong

Department of Food and Life Science

The Graduate School

Pukyong National University

February 2016

Protein tyrosine phosphatase 1B and α-glucosidase inhibitory activities of *Pueraria lobata* roots and its constituents

(갈근의 protein tyrosine phosphatase 1B 와 α-glucosidase 억제 활성)

Advisor: Prof. Jae Sue Choi

by

Su Hui Seong

A thesis submitted in partial fulfillment of the requirements

for the degree of

Master of Science

in Department of Food and Life Science, The Graduate School

Pukyong National University

February 2016

Protein tyrosine phosphatase 1B and α-glucosidase inhibitory activities of *Pueraria lobata* roots and its constituents

A dissertation

by

Su Hui Seong

Approved by:

_____

(Chairman) Taek Jeong Nam

_____ _____

(Member) Un Ju Jung (Member) Jae Sue Choi

February 26, 2016

Table of Contents

List of schemes

Scheme **Page**

List of figures

Figure **Page**

List of tables

Table **Page**

List of Abbreviations

ADT : autodock tools

CH_2Cl_2 : dichloromethane (methylene chloride)

DM : diabetic mellitus

DTT : dithiothreitol

EDTA : ethylenediamine tetraacetic acid

EtOAc : ethyl acetate

EtOH : ethanol

Fig. : figure

GA : genetic algorithms

GSK3 : glycogen synthase kinase-3

H_2O : water

Hz : herz (sec^{-1})

IC_{50} : 50% inhibitory concentration

IR : insulin receptor

IRS : insulin receptor substrates

***n*-BuOH** : ***n*-butanol**

***p*NPP** : ***p*-nitrophenyl phosphate**

***p*NPG** : ***p*-nitrophenyl alpha-D-glucopyranoside**

PI3K : phosphatidylinositol-3-kinase

PTP1B : protein tyrosine phosphatase 1B

PTPases : protein tyrosine phosphatases

RP : reverse phase

TLC : thin layer chromatography

UV : ultraviolet

갈근의 protein tyrosine phosphatase 1B 와 α-glucosidase 억제 활성

성 수 희

부경대학교 대학원 식품생명과학과

요 약

Protein tyrosine phosphatase 1B (PTP1B)는 인슐린 신호경로의 부정적인 조절자로 작용하고 α-glucosidase 는 탄수화물이 단당으로 분해되어 혈류로 흡수되는 작용에 중요한 역할을 한다. 그러므로, PTP1B와 α-glucosidase 의 저해제를 찾는 것은 당뇨병을 예방하는 것에 있어서 중요하다. 천연물로부터 저해제를 찾기 위한 계속된 연구 중에, 콩과식물에 속하는 갈근이 해열 작용과 알코올 중독에 대한 치료 효과로 전통적으로 천연 약재로 이용되어 왔으며, 특히 한방에서 소갈의 치료에 사용되었음에 주목하여 이번 연구에서는 갈근과 그 구성성분의 PTP1B와 α-glucosidase 억제 효과를 통해서 항당뇨 효과를 확인하였다. 갈근의 70 % 에탄올 추출물, 그 분획물 그리고 분리된 화합물들의 PTP1B와 α-glucosidase 저해 활성을 측정하였고 효소반응속도 연구와 분자적 도킹 시뮬레이션을 통해서 갈근으로부터 분리된 화합물들의 PTP1B와 α-glucosidase 저해제로서 이용될 가능성을 확인하였다. 여러가지 분획물들 중에서 *n*-hexane 분획물과 EtOAc 분획물이 높은 PTP1B 저해 활성을 보였고, CH_2Cl_2 분획물에서는 α-glucosidase 저해 활성이 가장 높게 나타났다. 특히, *n*-hexane 분획물에서 분리된 triterpenoids인 lupeol과 lupenone이 PTP1B를 효과적으로 저해하였고, 이들의 IC_{50}값은 각각 38.89 ± 0.17 그리고 15.11 ± 1.23 μM이였으며, 효소반응속도 연구를 통해 K_i 값이 각각 13.88 μM 그리고 21.24 μM인 비경쟁적 저해제임이 증명되었다. 게다가, 분자적 도킹 시뮬레이션에서 lupenone은 -8.53 kcal/mol의 결합 에너지를 가지고 lupenone의 케톤기의 산소원자가 PTP1B

의 활성 자리에 위치하는 CYS215와 ALA217 잔기와 상호작용하여 2개의 수소 결합을 형성하였고, 표준 리간드인 compound 23과 lupenone 모두 ALA217 잔기와 수소 결합을 형성함으로써 상호작용한다는 것은 주목할 만 하다. 반면에, lupeol은 -8.03 kcal/mol의 결합 에너지를 가지고, lupeol의 수산기의 산소원자가 PTP1B의 SER205 잔기와 하나의 수소 결합을 형성하였다. 이 결과를 통해서 수산기를 가지는 lupeol에 비해서 케톤기를 가지는 lupenone이 더 강한 PTP1B 저해 활성을 가진다는 것을 설명할 수 있다. EtOAc 분획물에서 분리된 daidzein과 genistein 그리고 CH_2Cl_2 분획물에서 분리된 calycosin에서 양성대조군인 acarbose보다 상당히 높은 α-glucosidase 저해 효과가 관찰되었고, 이들 화합물의 IC_{50}값은 각각 8.58 ± 0.94, 2.37 ± 0.52 그리고 6.84 ± 1.58 μM이였으며, 효소반응속도 연구를 통해 K_i 값이 각각 17.64, 5.03 그리고 13.83 μM인 비경쟁적 저해제로 조사되었다. 그리고, 분자적 도킹 시뮬레이션 결과는 이들 화합물이 각각 -7.16, -7.42 그리고 -7.31 kcal/mol의 결합 에너지 값을 가짐을 보여주었고, 표준 리간드인 α-D-glucose (-6.74 kcal/mol)보다 α-glucosidase와 더 많은 소수성 상호작용을 형성함으로써, 더 높은 결합 친화도를 가짐을 보여주었다. 결론적으로, triterpenoid인 lupenone과 lupeol은 강력한 PTP1B 저해 활성을 가지는 반면 isoflavone에 속하는 daidzein, genistein 그리고 calycosin은 두드러진 α-glucosidase 저해 활성을 나타냈으며, 효소반응속도 연구와 효소와 활성 화합물 간의 분자적 도킹 시뮬레이션은 이들 화합물에 대한 *in vitro* 실험 결과를 증명해 준다. 따라서, 이번 연구의 결과는 갈근과 그 구성 성분이 PTP1B와 α-glucosidase 억제 활성을 보여줌으로써, 항당뇨 효과를 가짐을 확인하였고, 갈근이 당뇨병 예방을 위한 기대되는 치료적 전략으로 이용될 가능성을 제시한다.

I. Introduction

Diabetic mellitus (DM) is a chronic disease caused by abnormal metabolism of fats, proteins and carbohydrates. Abnormal metabolism occurrs due to insulin deficiency and resistance. DM occurs all over the world, and its occurrence is significantly increasing in many countries (Parthasarathy et al, 2009). In 2013, 382 million adults aged 20-79 years in 174 countries had DM; this number is expected to reach 592 million by 2035. Most of DM sufferers live in countries of low- and middle-income and these will undergo considerable increase in case of DM over the following 22 years (Guariguata et al, 2014). Thus, treatment and prevention options for DM are necessary globally. The β-subunit of insulin receptor (IRβ) combined with insulin has intrinsic tyrosine kinase activity. Upon binding of insulin to α-subunit of insulin receptor, IRβ phosphorylates tyrosin residues of IR and then IR also phosphorylates insulin receptor substrate (IRS). Tyrosine-phosphorylated IRS also phosphorylates tyrosine residues of signaling molecules that draw its downstream effects, including the phosphatidylinositol-3-kinase (PI3K) and a serine-threonine kinase Akt. Activated Akt then phosphorylates the glycogen synthase kinase-3 (GSK3), and lead to increasing the number of GLUT4 transporters, and resulting in promotion of peripheral

glucose uptake (Qin et al, 2015). These pathways are in charge of metabolic insulin action. On the other hand, tyrosine-phosphorylated IRβ is also linked to Ras-mitogen-activated protein kinase (MAPK) pathway. This pathway is related to the regulation of some genes expression and controlling the cell growth and differentiation by cooperating with PI3K pathway (Patel et al, 2014). Insulin resistance is the key pathological characteristic of metabolic syndrome, which shows an unnatural insulin signaling pathway, including the IRβ, IRS1/2 and other downstream signal moledules involved in the malfunction of reversible phosphorylation of protein tyrosine and decreased insulin sensitivity of peripheral tissue (Ma et al, 2011). The protein-tyrosine phosphatases (PTPases) comprise a widespread homologous enzyme family that regulates cellular signal transduction and metabolism. The enzymes belonging to PTPase have been divided into two types, intracellular (nonreceptor type) and transmembrane (receptor type). Protein tyrosine phosphatase 1B (PTP1B) in involved in an intracellular group which acts as a major negative regulators of the insulin signaling containing IR and IRS by dephosphorylation of tyrosine-phosphorylated proteins (Goldstein, 2002; Gonza´lez-Rodríguez et al, 2010). Regulation of the signal transduction of insulin by PTP1B has been observed in both muscle and liver cell-lines. Insulin resistance is caused by disequilibrium in IR autophosphorylation and tyrosine kinase activity. Thus, overexpression of PTP1B has been detected in a state of insulin resistance. Moreover, PTP1B-

deficient mice exhibited not only lower serum insulin, triglyceride and blood glucose levels, but also activations of IR and an increase of insulin sensitivity, with no obvious disease phenotype and a normal fetal survival rate (Liu et al, 2015). Thus, PTP1B is expected to become a strong potential drug target for insulin sensitivity and insulin resistance. On the other hand, α-glucosidase is located in the intestinal brush-border surface membrane, which activates the final step of the digestive process. This enzyme is an exo-type carbohydrase and catalyzes the exohydrolysis of disaccharides including sucrose and maltose into absorbable monosaccharides such as glucose (Choi et al., 2010). Therefore, α-glucosidase inhibitors decrease the influx of glucose from the digestive tract to the blood stream. Acarbose, voglibose, and miglitol are well known α-glucosidase inhibitors, but these drugs are associated with side effects, such as adverse gastrointestinal symptoms, diarrhea and liver toxicity (Lordan et al., 2013). Therfore, natural α-glucosidase inhibitors with no ill or unwanted secondary effects are needed to treat DM.

Pueraria lobata (Willd.) Ohwi (Kudzu) is a leguminous vine native to much of eastern Asia, southeast Asia, and some Pacific islands, and it became known throughout the United States in 1876 (Prasain et al., 2003). The root of *P. lobata* is known as aka, kudzuvine, kudsu, nepalem, Japanese arrowroot, kuzu (Japanese), kudzu comun (Spanish), kopoubohne (German) and vigne japonaise

(French). The root of *P. lobata* well-known as Gegen in traditional Chinese (oriental) medicine has been used as a medicine, food ingredient, and fodder for many thousands of years. Moreover, the root of *P. lobata* was utilized earlier than other medicinal herbs in ancient China because it was used to treat wasting-thirst, which occurs due to dryness-heat and causes symptoms of rapid digestion with swift hunger and frequent urination (Cho et al, 2003). In addition, *P. lobata* root has anti-inflammatory, antioxidant (Jin et al, 2012), and antihypertensive activities and it is well known that efficacy of phytoestrogen and use in the treatment of alcoholism (Zhou et al, 2014). The root of *P. lobata* is a source of abundant polyphenolic compounds, including isoflavones such as puerarin, daidzein and genistein, isoflavonoid glycosides, puerarols and terpenoids such as lupenone and lupeol. Puerarin is the first compound isolated from the root of *P. lobata* and the most rich secondary metabolite (Wong et al, 2011). In prior studies, puerarin revealed potential preventative effect against coronary heart disease and hypoglycemic and hypolipemic effects on streptozotocin-diabetogenic mice by increasing insulin expression and preserving metabolic homeostasis. Because of this, many researchers have give attention to the amazing pharmacological activities of puerarin (Mun et al, 2015; Wu et al, 2013). Moreover, advanced glycation end products (AGEs) inhibitory activities of *P. lobata* and its constituents (Kim et al., 2006) have been reported. However, PTP1B and α-glucosidase inhibitory effects of the systematic extract as well as

the fractions and isolated compounds from the root of *P. lobata* and mechanisms of inhibition of PTP1B and α-glucosidase through enzyme kinetics and molecular docking simulation have not been reported. Thus, the aim of this study is to identify a natural herbal medicine for type 2 diabetes from the root of *P. lobata* via PTP1B and α-glucosidase inhibitions from the isolated compounds with enzyme kinetics and molecular docking simulation between the enzymes and active compounds.

II. Materials and methods

1. Plant materials

The root of *Pueraria lobata* was collected from the southern area of Gangwon-do Province, Korea, in March 2015 and authenticated by Professor Jae Sue Choi. A voucher specimen 20150320 was deposited in the authorized laboratory.

2. General experimental procedures

^{1}H-NMR and ^{13}C-NMR spectra were measured by a JEOL JNM ECP-400 spectrometer (Tokyo, Japan) at 400 MHz for ^{1}H-NMR and 100 MHz for ^{13}C NMR. UV lamp (Model ENF-240C, Spectroline, U.S.A.) with built in both of 365 nm and 245 nm UV light was used to search compounds on the TLC plates. PTP1B and α-glucosidase inhibitory activities were conducted using a microplate reader spectrophotometer (Molecular Devices, VERSA max, CA, USA).

3. Chemicals and reagents

Column packing meterials, silica (Si) gel 60 (70~230 mesh, Merck, Darmstadt, Germany), Sephadex LH-20 (bead size 25~100 μm, Merck, Germany), RP-18 (LiChroprep® RP-18, 40~63 μm, Merck, Germany) and Diaion HP-20 (250~850 μm, Sigma) were used for column chromatography. Thin layer chromatography was carried out using Kieselgel 60 F_{254} plates (20 × 20 cm, 0.25 mm, Merck) and RP-18 F_{254S} plates (5 × 10 cm, Merck) using 50 % H_2SO_4 as a spray reagent. Solvents used in extraction and column chromatography were of reagent grade, and were purchased from Sigma-Aldrich Co. or other commercial sources. Yeast α-glucosidase, acarbose, *p*-nitrophenyl phosphate (*p*NPP), *p*-nitrophenyl α-D-glucopyranoside (pNGP), ethylenediamine tetra acetic acid (EDTA), and dimethylsulfoxide (DMSO) were purchased from Sigma-Aldrich Co. (St. Louis, MO, USA). Protein tyrosine phosphatase 1B (PTP1B, human recombinant) and dithiothreitol (DTT) were purchased from Biomol® International LP (Plymouth Meeting, PA, USA) and Bio-Rad Laboratories (Hercules, CA, USA), respectively.

4. Experiment methods

4-1. Extraction and fractionation

The dried roots of *P. lobata* (3 kg) were extracted 5 times with 70% EtOH under reflux. The total filtrate was then concentrated to dryness *in vacuo* at 40 °C to give a 70% Ethanol (EtOH) extract (0.9 kg). For fractionation, 70% EtOH extract was suspended in H_2O and then successively partitioned three times with *n*-hexane, dichloromethane (CH_2Cl_2), ethyl acetate (EtOAc) and *n*-butanol (*n*-BuOH) in the ordered name to yield *n*-hexane fraction (27.5 g), CH_2Cl_2 fraction (4.3 g), EtOAc fraction (22.2 g), *n*-BuOH fraction (391 g) and H_2O fraction (455 g).

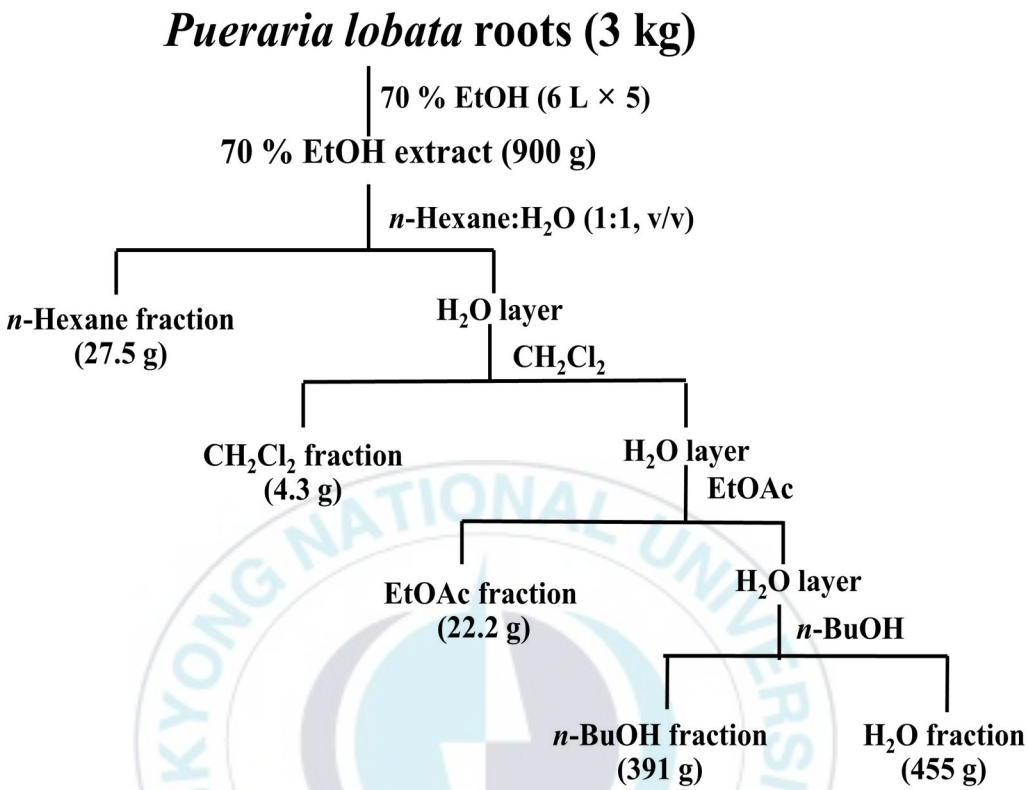

Scheme 1. Extraction and fractionation of *P. lobata* roots.

4-2. Isolation of compounds

4-2-1. Isolation of compounds from the *n*-hexane fraction

n-Hexane fraction (27.5 g) was chromatographed on silica gel (Si) column chromatography with *n*-hexane-EtOAc (30:1 to 2:1, gradient) solvent system to give 15 subfractions (fraction 1~15). Fraction 1 was chromatographed on Si gel column with *n*-hexane-EtOAc (100:1) to yield lupenone (234 mg). Successive recrystallization of 2 fractions from 100% MeOH yielded 2 compounds, lupeol (550 mg) from fraction 3 and β-sitosterol (350 mg) from fraction 5. Recrystallization of fraction 9 from 100% MeOH yielded puerarol (280 mg), tuberosin (10 mg) and coumesterol (20 mg). These compounds were isolated according to the method described by Jin et al. (2012), and were identified by spectroscopy including ^{1}H and ^{13}C-NMR, as well as by comparison with published spectral data. The structures are shown in Fig. 1.

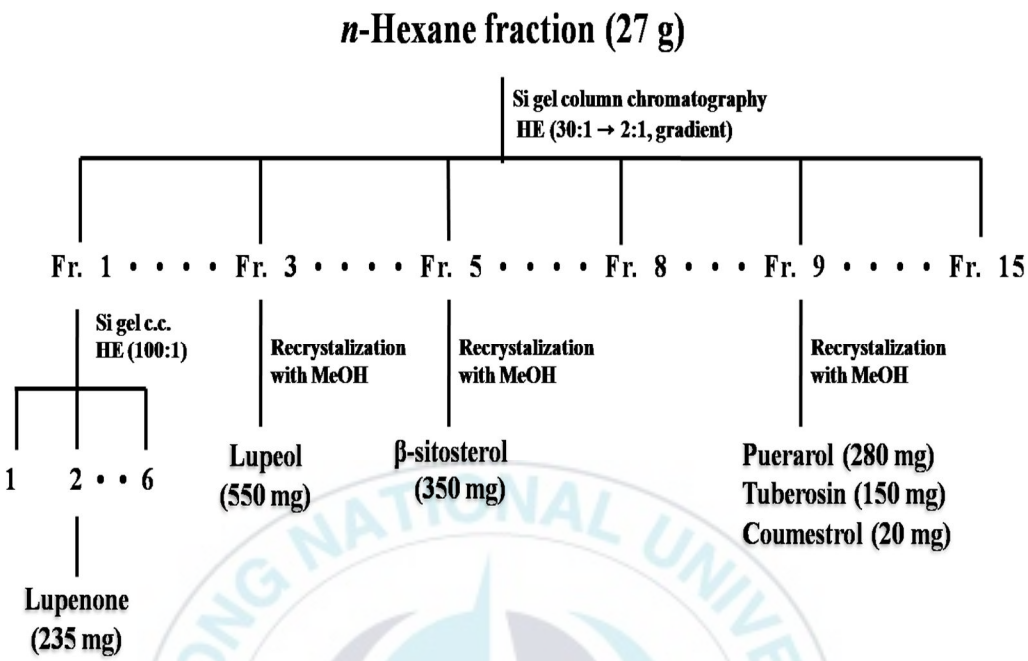

Scheme 2. Isolation of compounds from the *n*-hexane fraction of *P. lobata* roots.

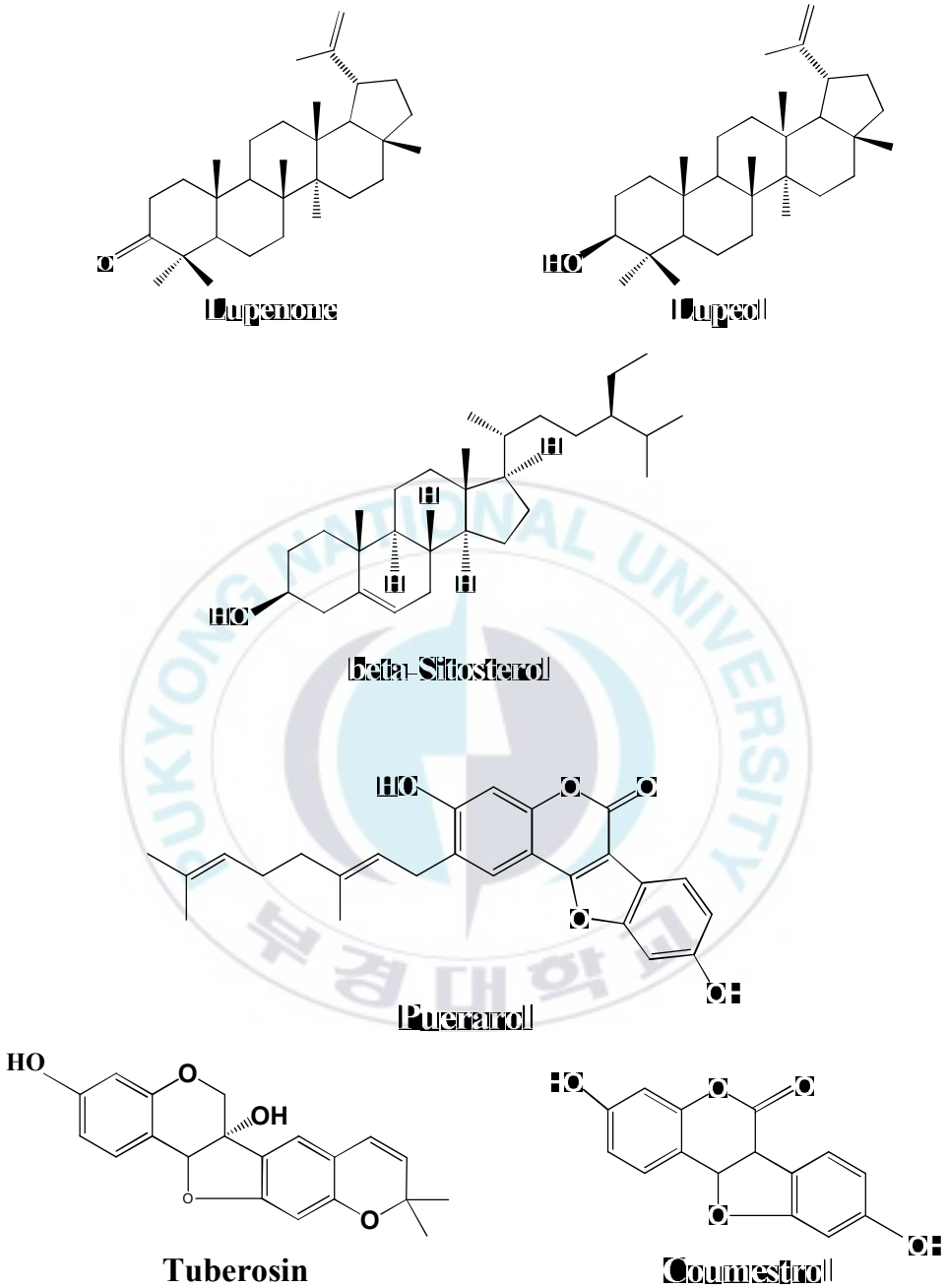

Fig. 1. Chemical structures of the compounds isolated from the *n*-hexane fraction of *P. lobata* roots.

4-2-2. Isolation of compounds from the CH_2Cl_2 fraction

CH_2Cl_2 fraction (4.3 g) was chromatographed on Si column chromatography with *n*-hexane-EtOAc (10:1 to 2:1, gradient) solvent system to give 10 subfractions (fraction 1~10). Fraction 7 was chromatographed on RP-18 column chromatography with 50% MeOH solvent system to give 2 compounds, puerarol (100 mg) and tuberosin (50 mg). Fraction 8 was chromatographed on Si column chromatography with CH_2Cl_2-MeOH (300:1) solvent system to give calycosin (40 mg). These compounds were isolated according to the method described by Jin et al. (2012), and were identified by spectroscopy including ^{1}H and ^{13}C-NMR, as well as by comparison with published spectral data. The structures are shown in Fig. 2.

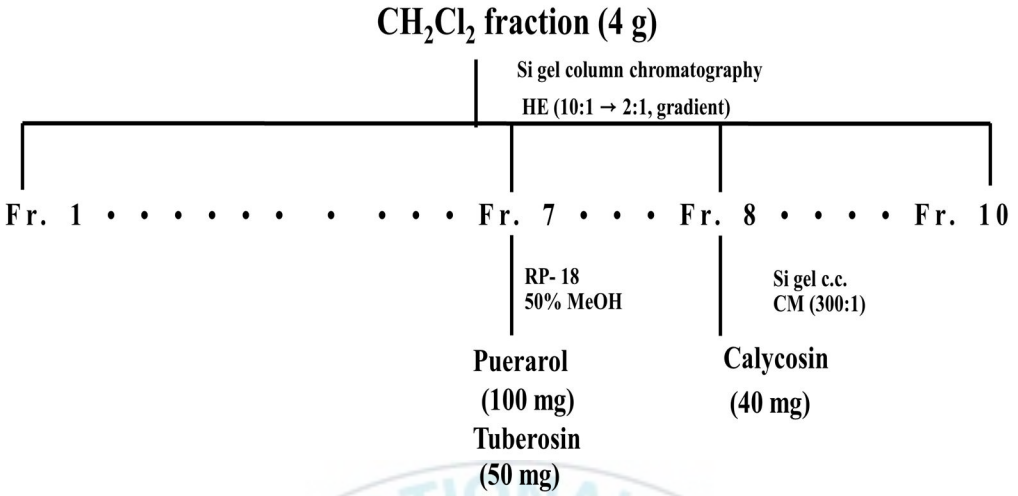

Scheme 3. Isolation of compounds from the CH_2Cl_2 fraction of *P. lobata* roots.

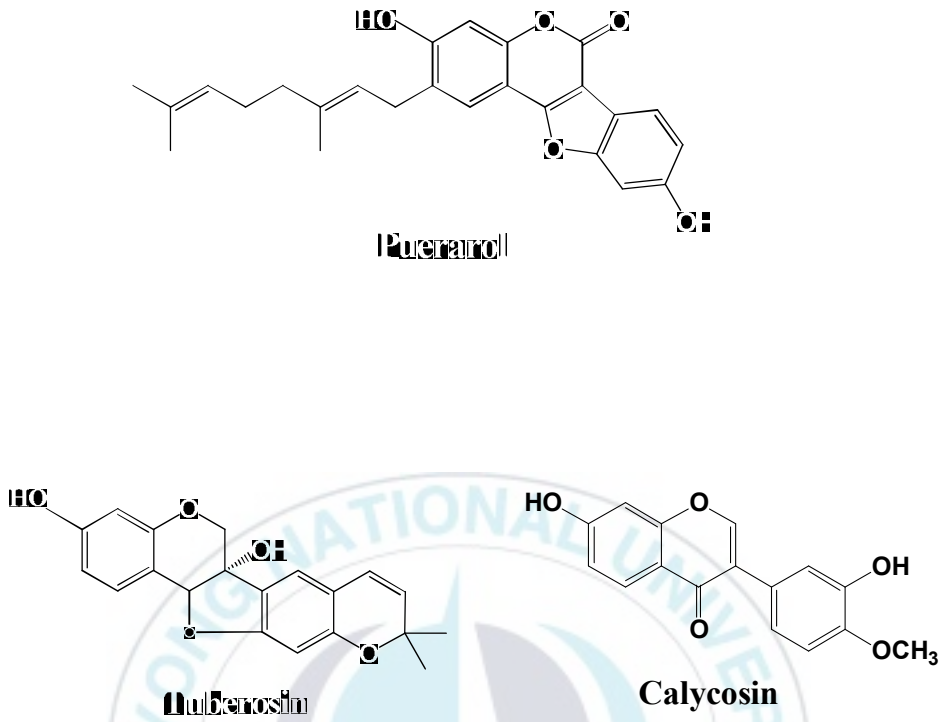

Fig. 2. Chemical structures of the compounds isolated from the CH_2Cl_2 fraction of *P. lobata* roots.

4-2-3. Isolation of compounds from the EtOAc fraction

EtOAc fraction (22.2 g) was chromatographed on Si column chromatography with CH_2Cl_2-MeOH (1:0 to 1:1, gradient) solvent system to give 14 subfractions (fraction 1~14). Fraction 10 was recrystallized from 100% MeOH resulted in the isolation of daidzein (1.2 g) and filtrate was chromatographed on Si column chromatography with CH_2Cl_2:MeOH (20:1, gradient), which resulted in the isolation of genistein (1 g). Fraction 12 was chromatographed on Sephadex LH20 with MeOH to give 12 subfractions (Sub-Fr.E-12-1~12). The combined Sub-Fr.E-12-8 and Sub-Fr.E-12-9 were chromatographed on Si column chromatography with CH_2Cl_2:MeOH:H_2O (5:1:0.1) resulted in the isolation of puerarin (1.05 g). Sub-Fr.E-12-10 was chromatographed on Si column chromatography with CH_2Cl_2:MeOH:H_2O (10:1:0.1) resulted in the isolation of (+)-Puerarol B-2-*O*-glucoside (115 mg). These compounds were isolated according to the method described by Jin et al. (2012), and were identified by spectroscopy including ^{1}H and ^{13}C-NMR, as well as by comparison with published spectral data. The structures are shown in Fig. 3.

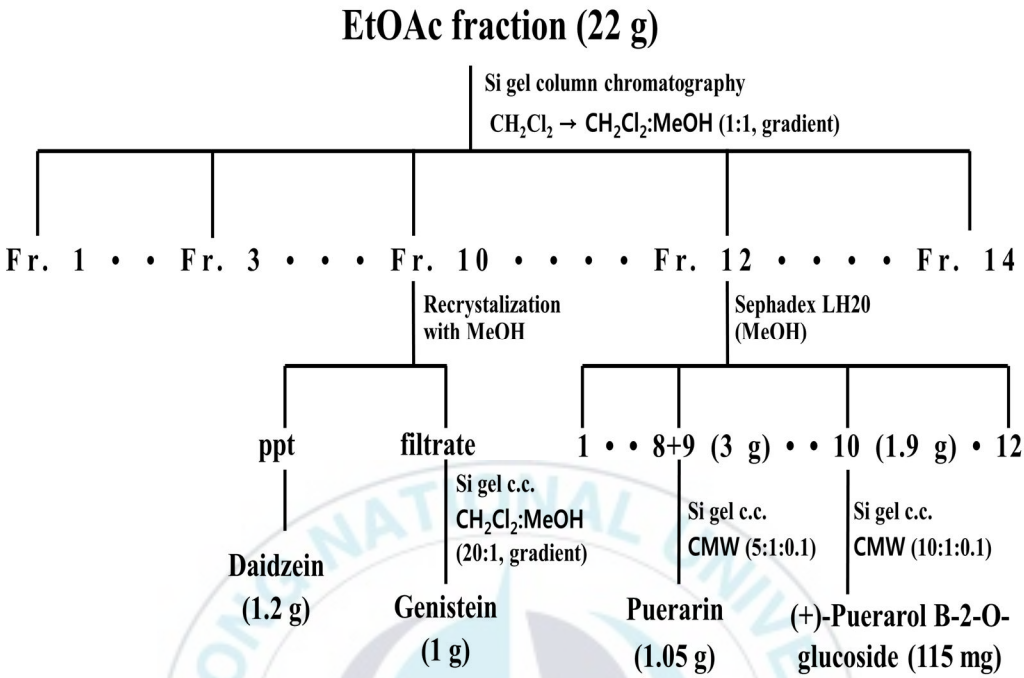

Scheme 4. Isolation of compounds from the EtOAc fraction of *P. lobata* roots.

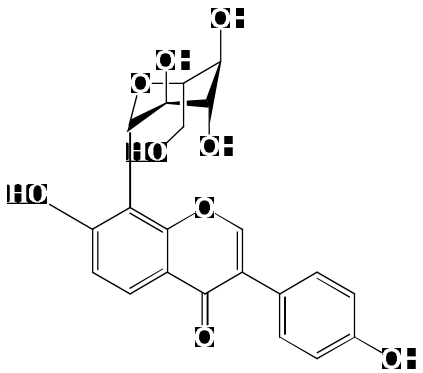

Puerarin

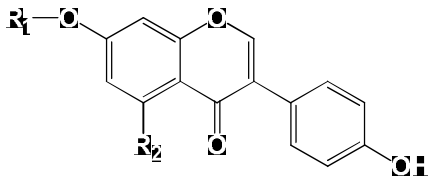

Daidzein : R_1=H R_2=H
Genistein : R_1=H R_2=OH

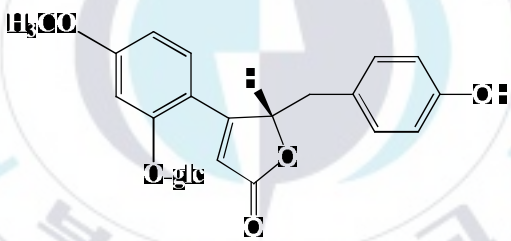

(E)-Puerarol B-2-O-glucoside

Fig. 3. Chemical structures of the compounds isolated from the EtOAc fraction of *P. lobata* roots.

4-2-4. Isolation of compounds from the *n*-BuOH fraction

n-BuOH fraction (391 g) was chromatographed on Diaion HP-20 with H_2O-MeOH solvent system to give H_2O (90 g), 40% MeOH (270 g), 60% MeOH (15 g) and MeOH (16 g) fractions. H_2O fraction was chromatographed on a Sephadex LH-20 with H_2O to give 11 fractions (Sub-Fr.B-1-1~11). Sub-Fr.B-1-3 was recrystallized with 100% MeOH, yielding allantoin (170 mg). Sub-Fr.B-1-4 was chromatographed on Si column chromatography with CH_2Cl_2:MeOH:H_2O (26:14:4) , followed by a RP-18 column with 10% MeOH resulted in the isolation of 3'-hydroxypuerarin (10 mg). The combined sub-Fr.B-1-5 and sub-Fr.B-1-6 were chromatographed on a Si column chromatography with CH_2Cl_2:MeOH:H_2O (26:14:4) resulted in the isolation of two compounds, daidzein-8-*C*-apiosyl-(1→6) glucoside (800 mg) and puerarin (12 g). Sub-Fr.B-1-11 was chromatographed on a Si column chromatography with CH_2Cl_2:MeOH:H_2O (26:14:4) resulted in the isolation of genistin (80 mg). 40% MeOH fraction was chromatographed on Si column chromatography with CH_2Cl_2:MeOH:H_2O (26:14:4) resulted in the isolation of 3'-methoxypuerarin (125 mg) and daidzin (3 g). 60% MeOH fraction was chromatographed on Si column chromatography with CH_2Cl_2:MeOH:H_2O (26:14:4) resulted in the isolation of daidzin (3 g). These compounds were isolated according to the method described by Jin et al. (2012), and were identified by spectroscopy including ^{1}H and ^{13}C-NMR, as well as by comparison

with published spectral data. The structures are shown in Fig. 4.

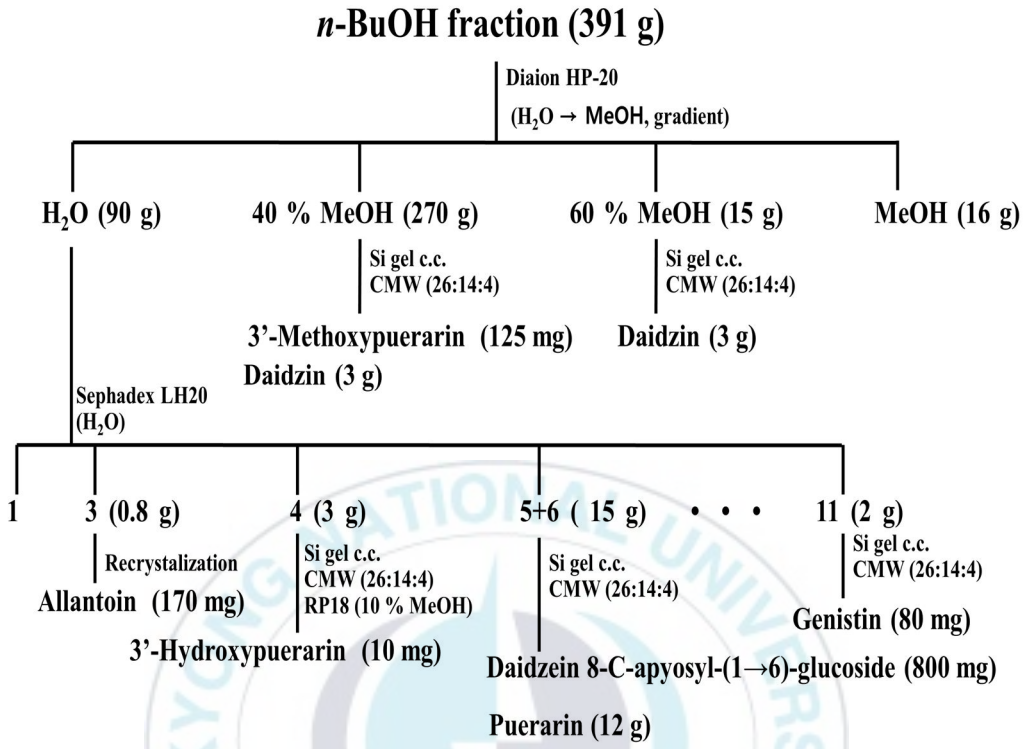

Scheme 5. Isolation of compounds from the *n*-BuOH fraction of *P. lobata* roots.

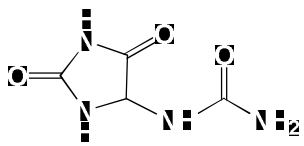

Allantoin

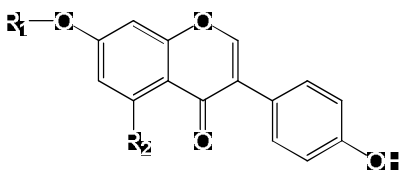

Daidzin : R_1=Glc R_2=H
Genistin : R_1=Glc R_2=OH

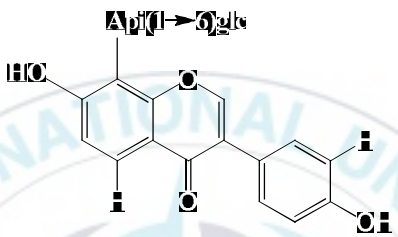

Daidzein 8-C-apiosyl-(1→6) glucoside

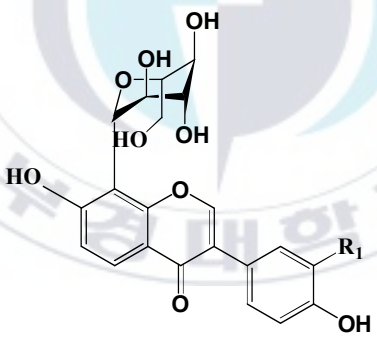

Puerarin : R_1=H
3'-Hydroxypuerarin : R_1=H
3'-Methoxypuerarin : R_1=OCH_3

Fig. 4. Chemical structures of the compounds isolated from the *n*-BuOH fraction of *P. lobata* roots.

4-3. Anti-diabetic experiments

4-3-1. Protein tyrosine phosphatase inhibitory assay

The human recombinant PTP1B inhibitory activities of the root of *P. lobata* and its constinuents were measured using reagent *p*NPP as substrate (Cui et al., 2006). To each well of a 96-well plate (final volume 100 μL), PTP1B enzyme diluted with PTP1B reaction buffer containing 50 mM citrate (pH 6.0), 0.1 M NaCl, 1 mM EDTA, and 1 mM DTT was added with or without a test sample. The plate was pre-incubated at 37 °C for 10 min, and then 50 μL of 2 mM *p*NPP in PTP1B reaction buffer was added. After incubation at 37 °C for 20min in the dark, the reaction was terminated by the addition of 10 M NaOH. The amount of *p*-nitrophenyl produced by enzymatic dephosphorylation of *p*NPP was estimated by measuring the absorbance at 405 nm using a microplate spectrophotometer (Molecular Devices, Sunnyvale, CA, USA). Non-enzymatic dephosphorylation of 2 mM *p*NPP was corrected by measuring the increase in absorbance at 405 nm in the absence of PTP1B enzyme. Ursolic acid was used as a positive control. The inhibition (%) was calculated by the following equation and the half maximal inhibitory concentration, IC_{50} is expressed as the mean ± S.E.M. of triplicate experiments.

$$\textbf{Inhibition (\%)} = \{1-(A_{Sample} - A_{Sample\text{-}C})/A_{Control}\} \times 100$$

A_{Sample} : The absorbance with sample.

$A_{Sample\,-\,C}$: The absorbance with sample in the absence of PTP1B enzyme

$A_{Control}$: The absorbance without sample

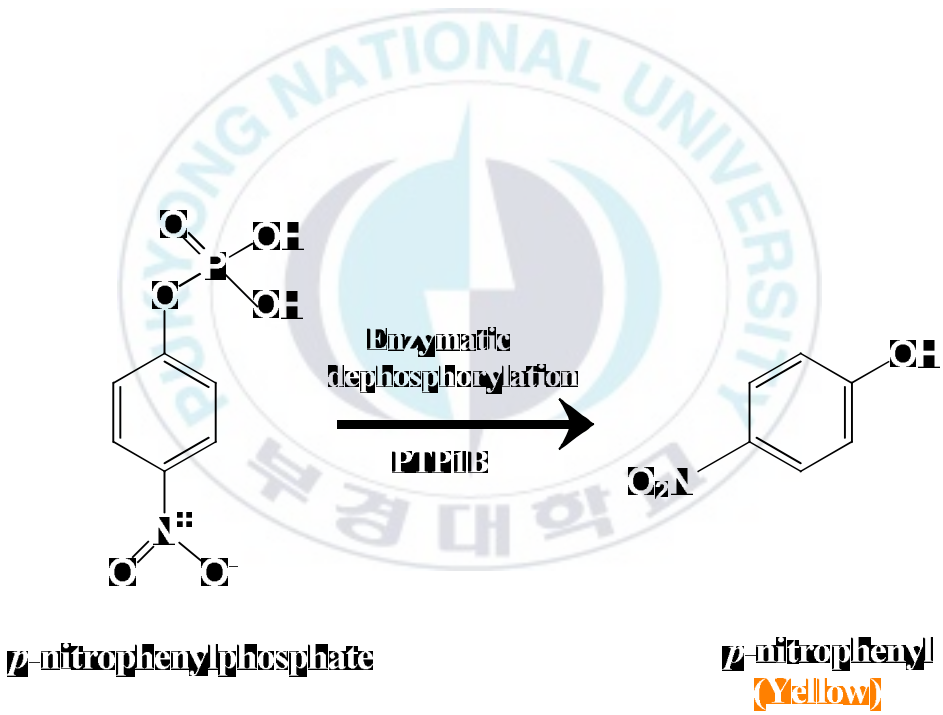

Fig. 5. Enzymetic dephosphorylation of *p*-nitrophenylphosphate by PTP1B.

4-3-2. α-Glucosidase inhibitory assay

The α-glucosidase inhibition study was carried out spectrophotometically in a 96-well microplate reader according to the modified method of Li et al. (2005). A total of 60 μL of a reaction mixture containing 20 μL of 100mM phosphate buffer (pH 6.8), 20 μL of 2.5 mM *p*NP,G and 20 μL of the test sample dissolved in 10 % DMSO were added to each well. After incubation at 37 ℃ for 5 min in the dark, 20 μL of α-glucosidase (0.2 U/mL) in 10 mM phosphate buffer (pH 6.8) was added. The plate was again incubated at 37 ℃ for 15 min in the dark, and then 80 μL of 0.2 M sodium carbonate solution was added to terminate the reaction. Immediately, the absorbance was read at 405 nm using a microplate spectrophotometer (Molecular Devices, Sunnyvale, CA, USA). The control contained the same reaction mixture except that the equivalent volume of 100 mM phosphate buffer was added in place of test sample solution. Acarbose was used as a positive control. The inhibition (%) was calculated by the following formula and 50 % inhibition concentration, IC_{50} is expressed as the mean ± S.E.M. of triplicate experiments.

$$\textbf{Inhibition (\%)} = \{1- (A_{Sample} - A_{Sample\text{-}C})/A_{Control}\} \times 100$$

A_{Sample} : The absorbance with sample.

$A_{Sample\text{-}C}$: The absorbance with sample in the absence of *p*NPG substrate

$A_{Control}$: The absorbance without sample

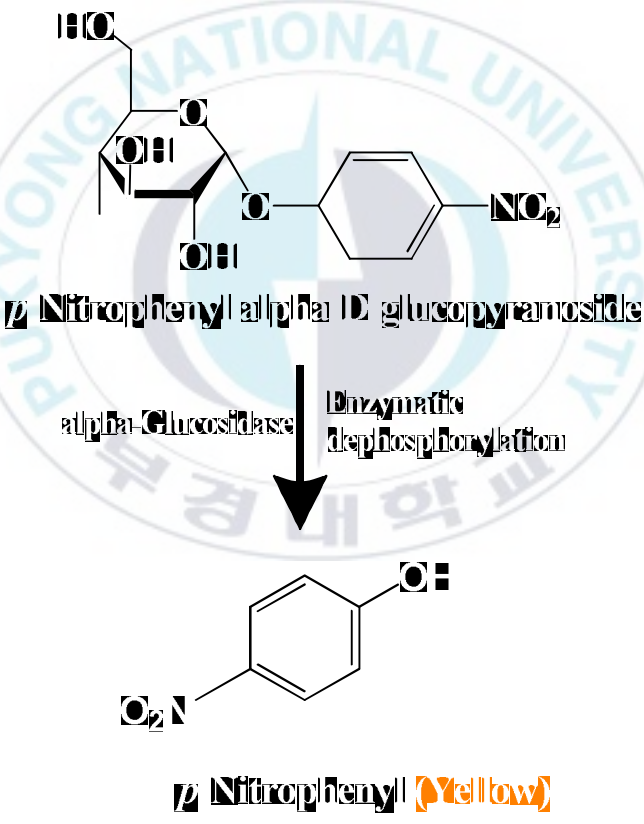

Fig. 6. Enzymatic dephosphorylation of *p*-nitrophenyl α-D-glucopyranoside by the α-glucosidase.

4-4. Enzyme kinetic analysis

4-4-1. Enzyme kinetic analysis with and PTP1B

In order to determine the inhibition mechanism, two kinetic methods using Lineweaver-Burk and Dixon plots were complementarily used (Lineweaver and Burk, 1934; Cornish-Bowden, 1974; Dixon, 1953). Each enzymatic inhibition at various concentrations of test samples was evaluated by monitoring the effect of different concentration of the substrate in Dixon plots (single reciprocal plot). Dixon plots for inhibition of PTP1B were obtained in the presence of different concentrations of *p*NPP substrate. Using Lineweaver-Burk double reciprocal plots, the PTP1B inhibition mode was determined at various concentration of *p*NPP substrate in the absence or presence of different test compounds concentration. The enzymatic procedures consisted of the same aforementioned PTP1B assay methods. The types of inhibition were determined by both methods, whereas inhibition constants (K_i) were determined by interpreting the Dixon plots, in which the value of the x-axis represents K_i.

4-4-2. Enzyme kinetic analysis with α-glucosidase

In order to determine the inhibition mechanism, two kinetic methods using Lineweaver-Burk and Dixon plots were complementarily used (Lineweaver and Burk, 1934; Cornish-Bowden, 1974; Dixon, 1953). Each enzymatic inhibition at various concentrations of test samples was evaluated by monitoring the effect of different concentration of the substrate in Dixon plots (single reciprocal plot). Dixon plots for inhibition of α-glucosidase were obtained in the presence of different concentrations of *p*NPG substrate: 0.625 mM, 1.25 mM and 2.5 mM. Using Lineweaver-Burk double reciprocal plots, the α-glucosidase inhibition mode was determined at various concentration of *p*NPG in the absence or presence of different test compounds concentration. The enzymatic procedures consisted of the same aforementioned α-glucosidase assay methods. The types of inhibition were determined by both methods, whereas inhibition constants (K_i) were determined by interpreting the Dixon plots, in which the value of the x-axis represents K_i.

4-5. Molecular docking simulation

4-5-1. Molecular docking simulation in PTP1B inhibition

X-ray crystallographic structures of PTP1B, with its potent and selective inhibitor compound 23 (PDB ID: 1NNY) were obtained from the RCSB Protein Data Bank (Bernstein et al., 1977, Berman et al., 2002) website at resolution of 2.40Å (Szczepankiewicz et al., 2003). This protein structure was regulated using the X-ray diffraction method. The reported heteroatom compound 23 and water molecules were removed from the protein structure for the docking simulation using Accelrys Discovery Studio 4.1 (http://www.accelrys.com; Accelrys, Inc. San Diego, CA, USA). The binding area of compound 23 of protein was considered to be the most convenient region for ligand binding in the docking simulation. The 3D structures of lupenone and lupeol were obtained from the Pubchem Compound (NCBI), with compound CIDs of 92158, 259846, respectively. Automated docking simulation was performed using Autodock tools (ADT) to assess the appropriate binding orientations and conformations of the ligand molecules with different protein inhibitors. A Lamarkian genetic algorithm method implemented in Autodock 4.2 was employed. For docking calculations, Gasteiger charges were added by default, the rotatable bonds were set by the Autodock tools, and all torsions were allowed to rotate. The grid maps were generated by the Autogrid program where the grid box size of 126 × 126 × 126

had a default spacing of 0.375 Å. The X, Y, Z center was 37.303, 30.97 and 33.501. The docking protocol for rigid and flexible ligand docking consisted of 10 independent Genetic Algorithms (GA), while other parameters were used as defaults of the ADTs. The binding aspect of PTP1B residues and their corresponding binding affinity score were regarded as the best molecular interaction. The results were analyzed using UCSF Chimera (Pettersen et al., 2004), while the hydrogen bond interacting residues and Van der Waals interacting residues were visualized by Ligplot.

4-5-2. Molecular docking simulation in α-glucosidase inhibition

The crystal structures of α-glucosidase used in biological assays from *Saccharomyces cerevisiae* yeast (PDB ID: 3A4A), with its known competitive inhibitor α-D-glucose were obtained from the RCSB Protein Data Bank website at resolution of 1.60Å (Yan et al, 2014). This protein structure was regulated using the X-ray diffraction method. The reported inhibitor α-D-glucose and water molecules were removed from the protein structure for the docking simulation using Accelrys Discovery Studio 4.1 (http://www.accelrys.com; Accelrys, Inc. San Diego, CA, USA). The binding area of α-D-glucose of protein was considered to be the most convenient region for ligand binding in the docking simulation. The 3D structures of daidzein, genistein, and calycosin were obtained from the Pubchem Compound (NCBI), with compound CIDs of 5281708, 5280961 and 5280448, respectively. Automated docking simulation was performed using Autodock tools (ADT) to assess the appropriate binding orientations and conformations of the ligand molecules with different protein inhibitors. A Lamarkian genetic algorithm method implemented in Autodock 4.2 was employed. For docking calculations, Gasteiger charges were added by default, the rotatable bonds were set by the Autodock tools and all torsions were allowed to rotate. The grid maps were generated by the Autogrid program where the grid box size of 126 × 126 × 126 points with a default spacing of 0.375 Å. The X, Y, Z

center was 21.272, -0.751 and 18.633, respectively. The docking protocol for rigid and flexible ligand docking consisted of 10 independent Genetic Algorithms (GA), while other parameters were used as defaults of the ADTs. The binding aspect of the α-glucosidase residues and their corresponding binding affinity score were regarded as the best molecular interaction. The results were analyzed using UCSF Chimera (http://www.cgl.ucsf.edu/chimera/, Pettersen et al., 2004), while the hydrogen bond interacting residues and Van der Waals interacting residues were visualized by Ligplot.

5. Statistics

Data are presented as the mean ± standard error of the mean (SEM) of at least four independent experiments. Statistical comparison between groups was performed using one-way ANOVA followed by Student's *t*-test.

III. Results

1. Anti-diabetic activity

1-1. PTP1B inhibitory activities of *P. lobata* roots and its constituents

As shown in Fig. 7, The 70% EtOH extract of *P. lobata* roots showed PTP1B inhibitory activiy in a dose dependent manner with an IC_{50} value of 384.21 ± 13.30 μg/mL. Since the 70% EtOH extract of *P. lobata* showed PTP1B inhibitory activity, it was further fractionated for detailed investigation. The 70% EtOH extract of the root of *P. lobata* was dissolved in H_2O successively partitioned with *n*-hexane, CH_2Cl_2, EtOAc, and *n*-BuOH to obtain different solvent-soluble fractions. PTP1B inhibitory activity of the individual fractions of the root of *P. lobata* were then evaluated. Among the five solvent soluble fractions of the 70% EtOH extract, the *n*-hexane and EtOAc fractions showed potent PTP1B inhibitory potential with IC_{50} values of 12.43 ± 0.16 and 9.97 ± 0.65 μg/mL, respectively. The CH_2Cl_2 and *n*-BuOH fractions showed moderate inhibitory activities with IC_{50} values of 85.68 ± 6.29 and 118.20 ± 8.09 μg/mL. However, the H_2O fraction showed no activity under the concentration of 800 μg/mL (Table 1). Of the isolated compounds, lupeol and lupenone belonging to triterpenoids showed most

potent PTP1B inhibitory activity with respective IC_{50} values of 38.89 ± 0.17 and 15.11 ± 1.23 μM, and puerarol and tuberosin significantly inhibited PTP1B with IC_{50} values of 110.65 ± 3.81 and 183.95 ± 2.27 μM, respectively. Calycosin isolated from the CH_2Cl_2 fraction; and daidzein, genistein, puerarin and puerarol B-2-*O*-glucoside isolated from the EtOAc fraction were exhibited good inhibitory activities with IC_{50} values of 273.23 ± 1.85, 145.15 ± 2.36, 207.00 ± 13.47, 115.81 ± 1.72 and 258.15 ± 0.33 μM, respectively. Moreover, daidzin, genistin, 3'-methoxypuerarin and daidzein 8*C*-apiosyl (1→6) glucoside isolated from the *n*-BuOH fraction also showed high inhibitory activities with IC_{50} values of 207.68 ± 0.45, 157.30 ± 1.74, 175.09 ± 3.60 and 222.73 ± 3.59 μM, respectively. But, coumestrol, 3'-hydroxypuerarin and allantoin exhibited marginal PTP1B inhibitory activities with IC_{50} values of 415.52 ± 18.81, 573.38 ± 12.04 and 1078 ± 12.97 μM, respectively (Table 2).

1-2. α-Glucosidase inhibitory activities of *P. lobata* roots and its constituents

The 70% EtOH extract of *P. lobata* roots showed dose dependent α-glucosidase inhibitory activiy with an IC_{50} value of 531.24 ± 7.95 μg/mL. Among the five solvent soluble fractions of the 70% EtOH extract, the CH_2Cl_2 fraction showed

highest α-glucosidase inhibitory activity compared to the other fractions with an IC_{50} value of 1.96 ± 0.10 μg/mL. The *n*-hexane and EtOAc fractions also showed high inhibitory activities with respective IC_{50} values of 37.35 ± 1.90 and 40.39 ± 1.89 μg/mL. However, the *n*-BuOH fraction showed moderate activity with an IC_{50} value of 596.92 ± 1.24 μg/mL and the H_2O fraction showed no activity under the concentration of 1000 μg/mL (Table 1). Strong α-glucosidase inhibitory activity was observed at lupenone, lupeol and puerarol from the *n*-hexane fraction; calycosin and tuberosin from the CH_2Cl_2 fraction; and daidzein, genistein and puerarin from the EtOAc fraction. These compounds has higher activities with IC_{50} values ranging between 2.37 ± 0.52 and 176.35 ± 0.21 μM compared to positive control acarbose (IC_{50} = 144.26± 10.49 μM). Especially, daidzein, genistein and calycosin belonging to isoflavone showed notable inhibitory activities (IC_{50} values of 8.58± 0.94, 2.37 ± 0.52 and 6.84 ± 1.58 μM, respectively). In addition, puerarol B-2-*O*-glucoside, daidzin and coumestrol showed moderate α-glucosidase inhibitory activity with IC_{50} values of 609.43 ± 1.78, 485.73 ± 2.81 and 495.03 ± 2.99 μM, respectively. However, the rest of the compounds showed no α-glucosidase inhibitory effects under the tested concentrations (Table 2).

Table 1. Protein tyrosine phosphatase 1B and α-glucosidase inhibitory activities of the 70% EtOH extract and its various solvent soluble fractions of *P. lobata* roots

	IC_{50} (Mean ± SEM)	
	PTP1B[a]	α-Glucosidase[b]
70% EtOH extract	384.21 ± 13.30	531.24 ± 7.95
n-Hexane fraction	12.43 ± 0.16	37.35 ± 1.90
CH_2Cl_2 fraction	85.68 ± 6.29	1.96 ± 0.10
EtOAc fraction	9.97 ± 0.65	40.39 ± 1.89
n-BuOH fraction	118.20 ± 8.09	596.92 ± 1.24
H_2O fraction	> 800	> 1000
Ursolic acid[c]	1.77 ± 0.08	
Acarbose[d]		92.54 ± 2.16

[a, b] The 50 % inhibitory concentration (IC_{50}) values (μg/mL) were calculated from a log dose inhibition curve and are expressed as mean ± standard error of the mean (SEM) of triplicate experiments.[c, d] Positive control.

Table 2. PTP1B and α-glucosidase inhibitory activities of compounds from *P. lobata* roots

	IC_{50} (Mean ± SEM)	
	PTP1B[a]	α-Glucosidase[b]
Daidzein	145.15 ± 2.36	8.58 ± 0.94
Genistein	207.00 ± 13.47	2.37 ± 0.52
Puerarin	115.81 ± 1.72	147.30 ± 1.33
Puerarol B-2-*O*-glucoside	258.15 ± 0.33	609.43 ± 1.78
Allantoin	1078.04 ± 12.97	> 1500
3'-Hydroxypuerarin	573.38 ± 12.04	> 1500
Daidzein 8*C*-apiosyl (1→6) glucoside	222.73 ± 3.59	> 1500
3'-Methoxypuerarin	175.09 ± 3.60	> 1500
Daidzin	207.68 ± 0.45	485.73 ± 2.81
Genistin	157.30 ± 1.74	> 1500
Lupeol	38.89 ± 0.17	176.35 ± 0.21
Lupenone	15.11 ± 1.23	112.36 ± 0.18
Puerarol	110.65 ± 3.81	50.70 ± 1.53
Coumestrol	415.52 ± 18.81	495.03 ± 2.99
Tuberosin	183.95 ± 2.27	28.07 ± 3.10
Calycosin	273.23 ± 1.85	6.84 ± 1.58
Ursolic acid[c]	6.84 ± 0.13	
Acarbose[d]		144.26 ± 10.49

[a, b] The 50 % inhibitory concentration (IC_{50}) values (μM) were calculated from a log dose inhibition curve and are expressed as mean ± SEM of triplicate experiments. [c, d] Positive controls.

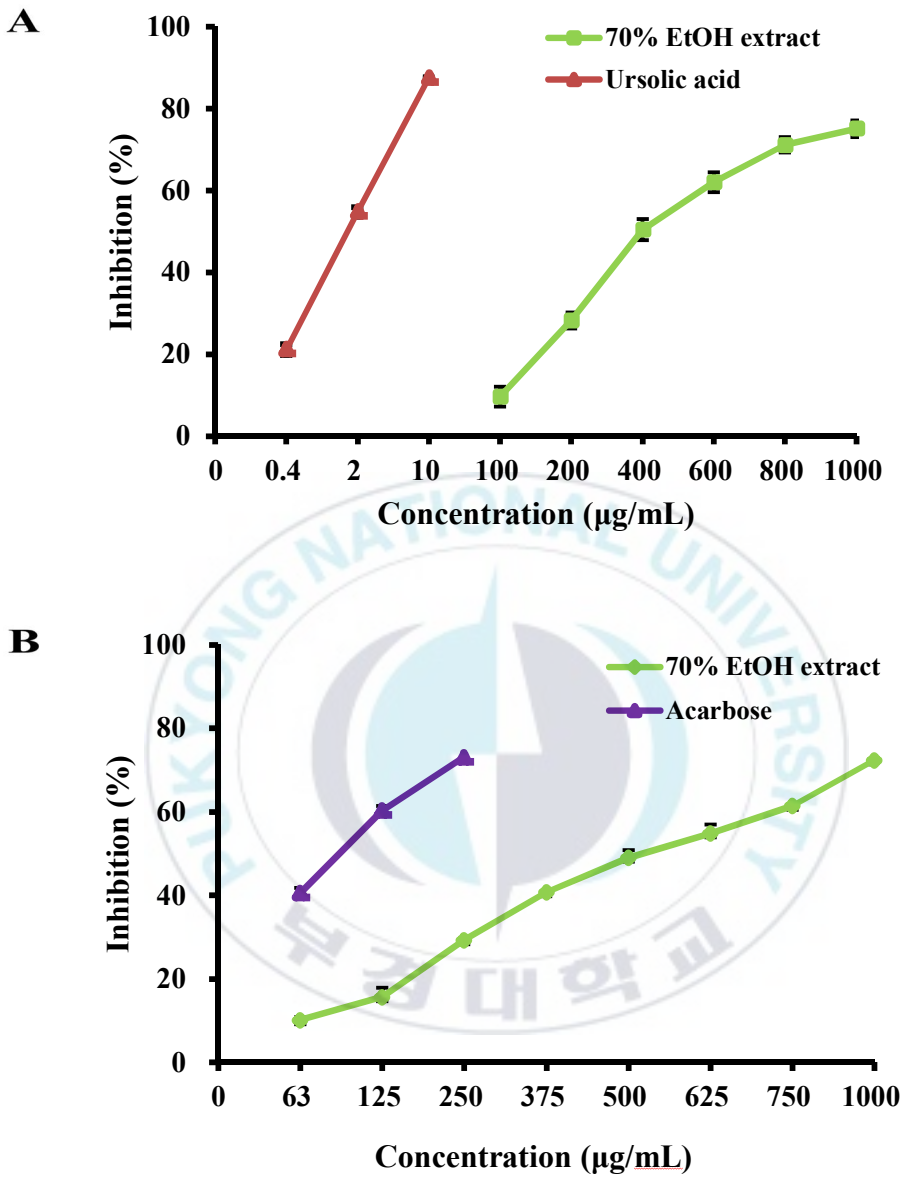

Fig. 7. (A) Protein tyrosine phosphatase 1B and (B) α-glucosidase inhibitory activities of the 70 % EtOH extract from *P. lobata* roots. Error bar indicates standard error of the mean (SEM).

2. Enzyme kinetic analysis

2-1. Enzyme kinetic analysis of active compounds from *P. lobata* roots with PTP1B

Among the compounds isolated from *P. lobata* roots, active compounds were analyzed to identify the correlation of compounds with substrate *p*NPP in PTP1B. Lineweaver-Burk plots were used to determine the type of inhibition and the inhibition constant (*Ki*) was determined using Dixon plots. Since daidzein, genistein, daidzin, genistin, lupenone and lupeol were showed high inhibitory activity compared with other compounds, these six compounds were investigated using the enzyme kinetic study. According to the Lineweaver-Burk plots based on PTP1B kinetic experiments, these 6 compounds showed noncompetitive-type inhibition against PTP1B that reduces the V_{max} values without changing the K_m values. Moreover, the Dixon plots showed *Ki* values of 30.75, 20.04, 105.84, 33.81, 13.88 and 21.24 μM, respectively (Fig. 8, 9, 10 and Table 3). Since the *Ki* value represents the concentration needed to combine the inhibitor with PTP1B enzyme, compounds with a lower *Ki* value were generally more effective inhibitors against PTP1B. Following the results, lupenone and lupeol possess notable *Ki* and IC_{50} values. In addition, daidzein and genistein belonging to isoflavone have more low *Ki* values than daidzin and genistin belonging to

isoflavonone glycoside.

2-2. Enzyme kinetic analysis of active compounds from *P. lobata* roots with α-glucosidase

Among the several compounds isolated from *P. lobata* roots, active compounds were analyzed to identify the correlation of compounds with substrate *p*NPG in α-glucosidase. Lineweaver-Burk plots were used to determine the type of inhibition and the inhibition constant (*Ki*) was determined using Dixon plots. Since daidzein, genistein and calycosin were showed significantly high inhibitory activities in comparison with positive control acarbose, these three compounds were investigated using the enzyme kinetic study. According to the Lineweaver-Burk plots based on α-glucosidase kinetic experiments, these three compounds showed noncompetitive-type inhibition against α-glucosidase that reduces the V_{max} values without changing the K_m values. Moreover, the Dixon plots showed *Ki* values of 17.64, 5.03 and 13.83 μM, respectively (Fig. 11 and Table 4). Since the *Ki* value represents the concentration needed to combine the inhibitor with α-glucosidase enzyme, compounds with a lower *Ki* value were generally more effective inhibitors against α-glucosidase.

Table 3. Enzyme kinetic analysis of compounds from *P. lobata* roots with PTP1B

Test compounds	*Ki* (μM) value [a]	Inhibition mode [b]
Daidzein	30.75	Noncompetitive
Genistein	20.04	Noncompetitive
Daidzin	105.84	Noncompetitive
Genistin	33.81	Noncompetitive
Lupenone	13.88	Noncompetitive
Lupeol	21.24	Noncompetitive

[a] Determined by Dixon plots. [b] Determined by Lineweaver-Burk plots.

Table 4. Enzyme kinetic analysis of compounds from *P. lobata* roots with α-glucosidase

Test compounds	*Ki* (μM) value [a]	Inhibition mode [b]
Daidzein	17.64	Noncompetitive
Genistein	5.03	Noncompetitive
Calycosin	13.83	Noncompetitive

[a] Determined by Dixon plots. [b] Determined by Lineweaver-Burk plots.

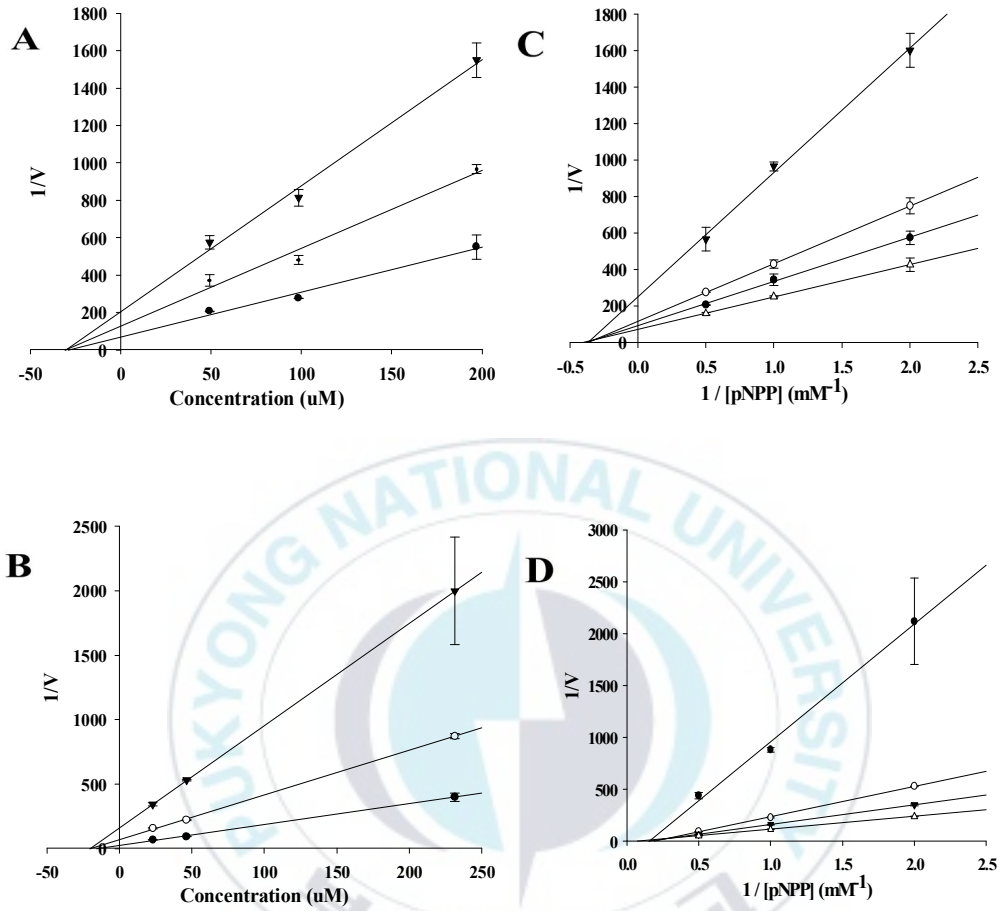

Fig. 8. Dixon and Lineweaver-Burk plots of the inhibition of PTP1B by daidzein and genistein. The results showed the effects of the presence of different concentrations of the substrate (2.0 mM (●), 1.0 mM (○), 0.5 mM (▼)) for (A) daidzein and (B) genistein and the effect of the presence of different concentrations of (C) daidzein (0 μM (△), 49.21 μM (●), 98.43 μM (○), 196.85 μM (▼)) and (D) genistein (0 μM (△), 23.15 μM (▼), 46.30 μM (○), 231.48 μM (●)). Error bar indicates SEM.

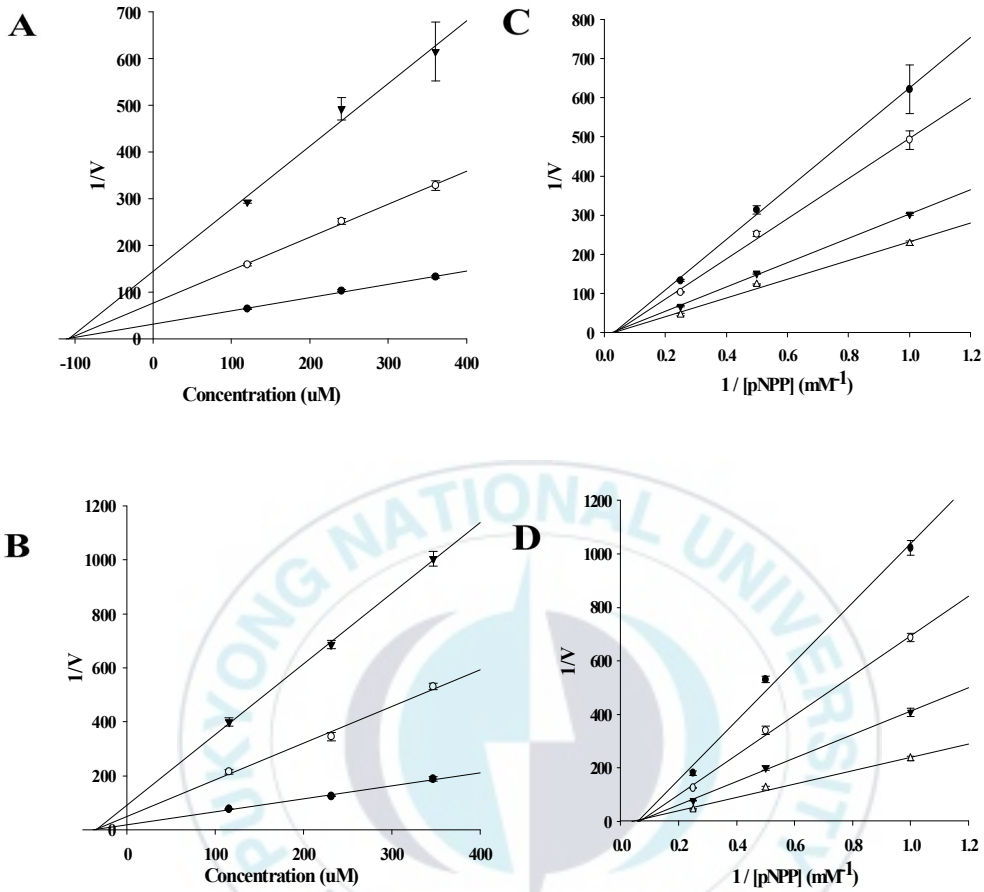

Fig. 9. Dixon and Lineweaver-Burk plots of the inhibition of PTP1B by daidzin and genistin. The results showed the effects of the presence of different concentrations of the substrate (4.0 mM (●), 2.0 mM (○), 1.0 mM (▼)) for (A) daidzin and (B) genistin and the effect of the presence of different concentrations of (C) daidzin (0 μM (△), 120.19 μM (▼), 240.38 μM (○), 360.58 μM (●)) and (D) genistin (0 μM (△), 115.74 μM (▼), 231.48 μM (○), 347.22 μM (●)). Error bar indicates SEM.

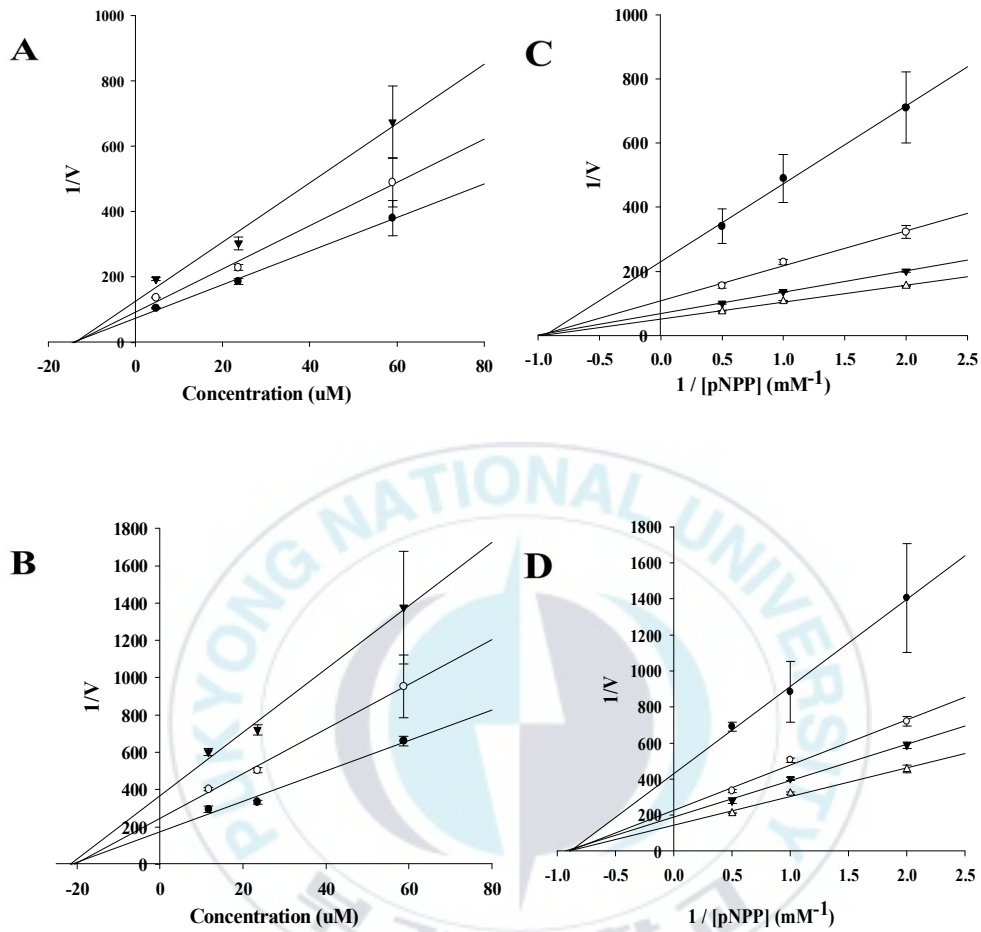

Fig. 10. Dixon and Lineweaver-Burk plots of the inhibition of PTP1B by lupeol and lupenone. The results showed the effects of the presence of different concentrations of the substrate (0.5 mM (▼), 1mM (○), 2mM (●)) for (A) lupeol and (B) lupenone and the effect of the presence of different concentrations of (C) lupeol (0 μM (△), 4.72 μM (▼), 23.58 μM (○), 58.96 μM (●)) and (D) lupenone (0 μM (△), 11.74 μM (▼), 23.47 μM (○), 58.69 μM (●)). Error bar indicates SEM.

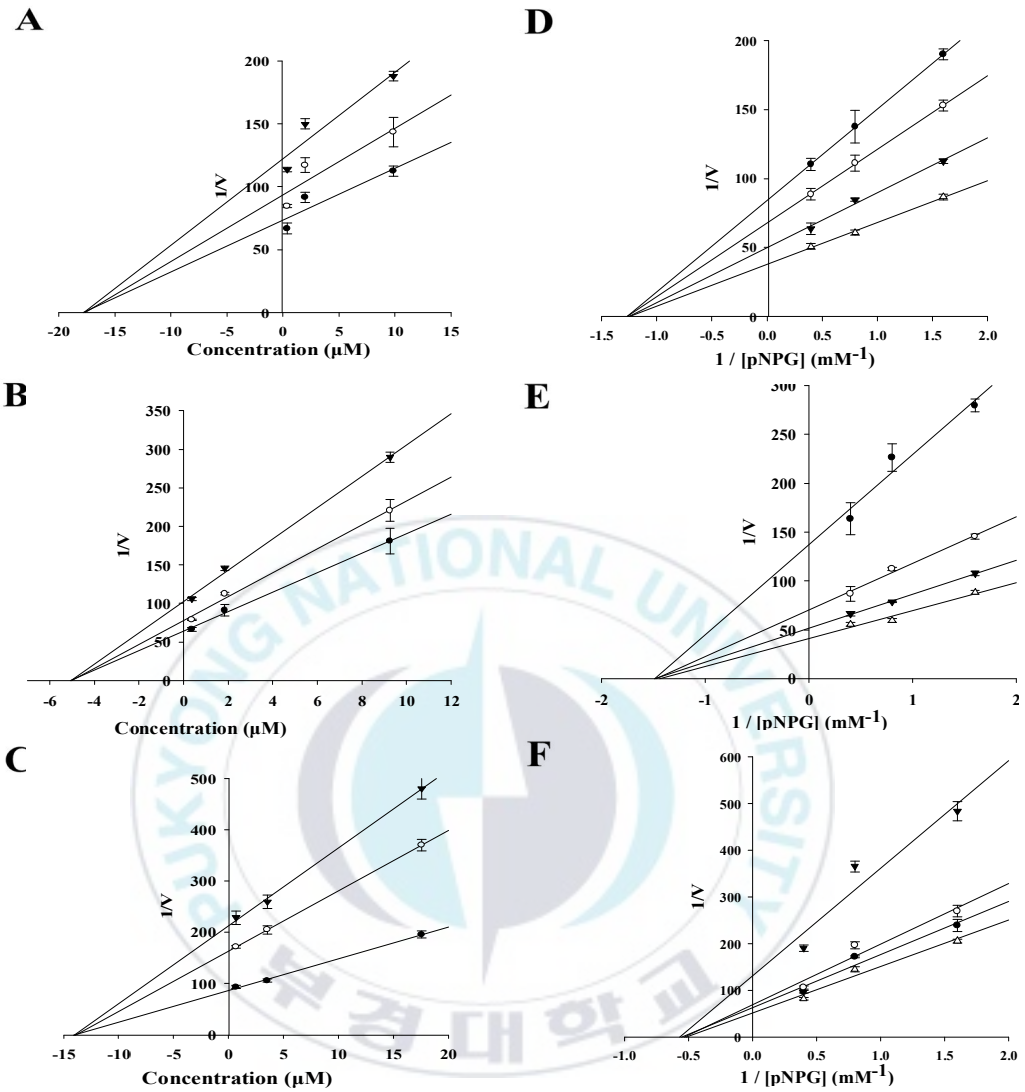

Fig. 11. Dixon and Lineweaver-Burk plots of the inhibition of α-glucosidase by daidzein, genistein, and calycosin. The results showed the effects of the presence of different concentrations of the substrate (0.625 mM (▼), 1.25 mM (○), 2.5 mM (●)) for (A) daidzein, (B) genistein, and (C) calycosin and the effect of the presence of different concentrations of (D) daidzein (0 μM (△), 0.39 μM (●), 1.97 μM (○), 9.84 μM (▼)), (E) genistein (0 μM (△), 0.37 μM (▼), 1.85 μM (○), 9.26 μM (●)), and (F) calycosin (0 μM (△), 0.70 μM (●), 3.52 μM (○), 17.59 μM (▼)). Error bar indicates SEM.

3. Molecular docking simulation study

3-1. Molecular docking simulation in PTP1B inhibition

To understand protein-ligand interaction geometrics at molecular level, molecular docking simulation is a good choice. In these studies, lupenone and lupeol with PTP1B molecular docking simulation was performed, where compound 23 was considered as the standard ligand for validating the Autodock 4.2 results. The binding energy of lupenone and lupeol with interacting residues including H-bond interacting residues and Van der Waals interacting residues along with number of H-bonds are listed in Table 5. The simulation results of Autodock 4.2 simulation are shown in Fig. 14, and the PTP1B-lupenone inhibitor complex showed a -8.53 kcal/mol binding energy with two hydrogen bonds with interacting residues of CYS215 and ALA217. The sulfur group (SG) of CYS215 and the nitrogen group (NG) of ALA217 were involved in the strong hydrogen bonding interaction with the oxygen (O1) of lupenone with bond distances of 3.00 and 3.19 Å, respectively. In addition, hydrophobic interactions were also observed between SER216, LYS116, ASP181, GLY183, PHE182, THR263, ASP265, ARG221, GLN266 and GLY220. All of these hydrophobic interactions are important to strengthening the protein-ligand interaction and for positioning of lupenone in the catalytic pocket in order to inhibit the activity of PTP1B. The molecular docking results were in good agreement with the experimental data. In

comparison, the lupeol binding affinity with PTP1B was -8.03 kcal/mol for one hydrogen bond. The SER205 residue is involved with a strong hydrogen bond with an oxygen (O1) of lupeol having a 2.81 Å bond distance. In addition, some hydrophobic interactions were involved with ILE281, PHE280, ARG199, GLY202, GLU200, and PHE196 interacting residues. These interactions may provide further stability to the lupeol-PTP1B complex and may help lupeol fit well in the active site pocket of PTP1B. Thus, the hydrogen bond and hydrophobic interactions from PTP1B might be involved in the hydrolysis of substrate molecules. The molecular docking result of PTP1B was in close agreement with the experimental data with respect to the inhibition activity by lupeol.

Table 5. Molecular interaction results of the PTP1B active sites with the known inhibitor (compound 23), lupenone and lupeol

Compound	Binding energy [a] (kcal/mol)	No. of H-bonds	H-bond interacting residues [b]	Van der Waals bond interacting residues [c]
Compound 23	-10.18	11	SER216,ARG221, ALA217,ILE219, GLY220, ARG24, ARG254, ASP48	TYR46,LYS120,THR263, CYS215,CLN266,VAL149, MET25,GLN262,ASP29, ARG24,SER28
Lupenone	-8.53	2	CYS215, ALA217	SER216, LYS116,ASP181, GLY183,PHE182,THR263, ASP265,ARG221,GLN266, GLY220
Lupeol	-8.03	1	SER205	ILE281,PHE280,ARG199, GLY202,GLU200,PHE196

[a] The semi-empirical free-energy force field was used to predict the binding free energies of protein-ligand complexes of a known structure and the binding energies of both the bound and unbound states. [b, c] All amino acid residues were located 3.75 Å from the original enzyme/inhibitor complex in the Autodock 4.2 program.

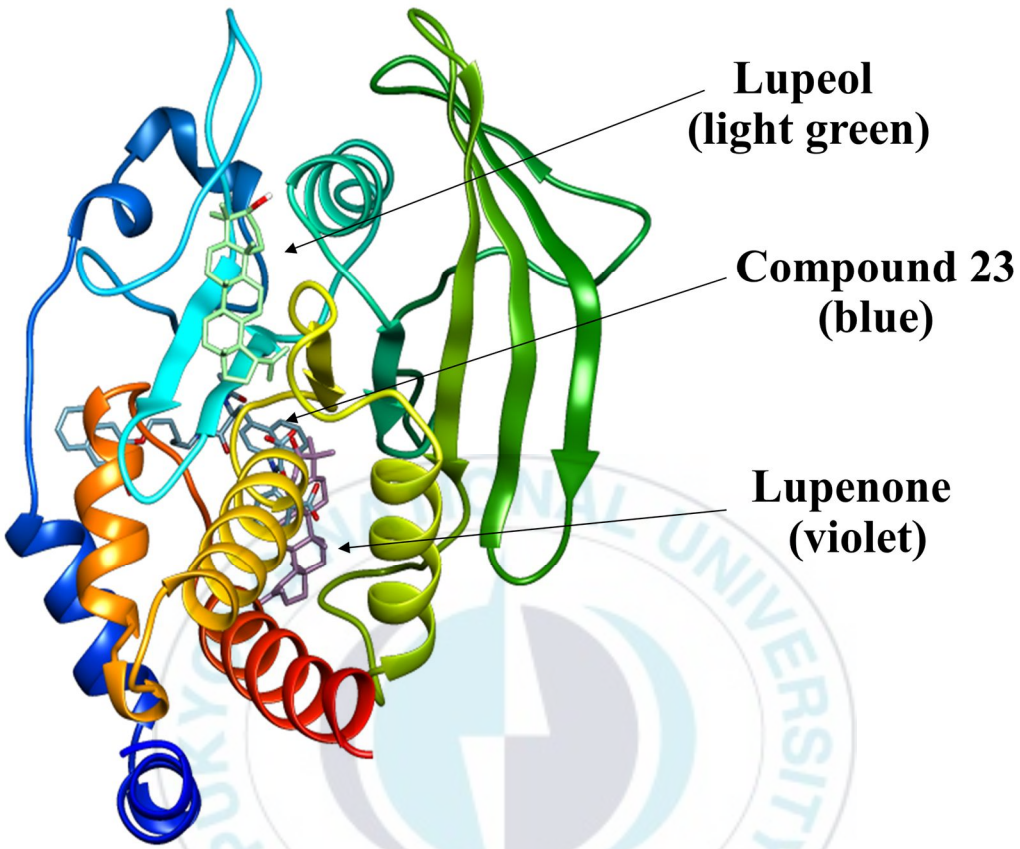

Fig. 12. Molecular docking models of the PTP1B inhibition of compound 23, lupeol and lupenone.

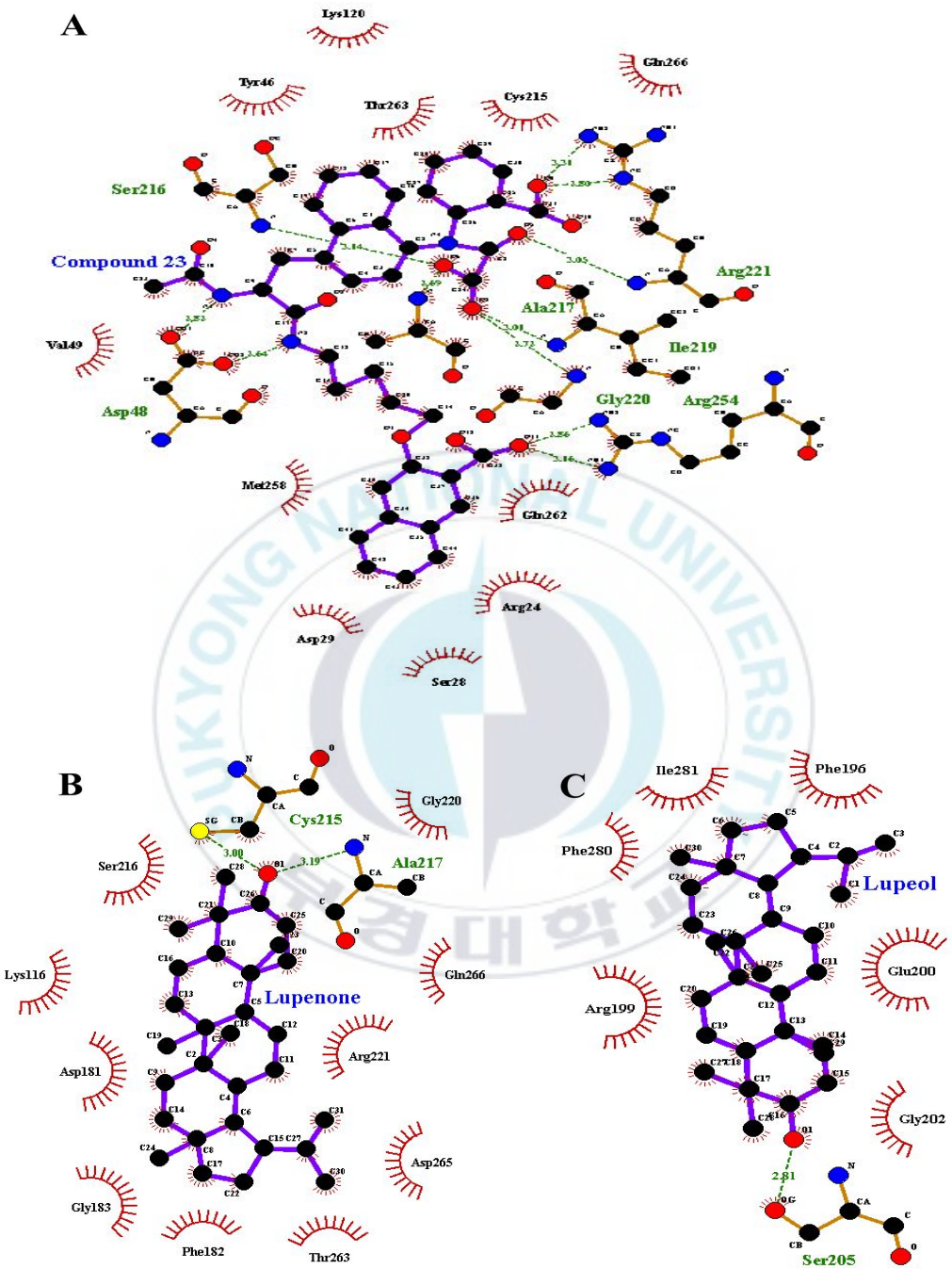

Fig. 13. Ligand interaction diagram of PTP1B inhibition of (A) compound 23, (B) lupeol, and (C) lupenone.

3-2. Molecular docking simulation in α-glucosidase inhibition

In this molecular docking simulation, daidzein, genistein, and calycosin with α-glucosidase were analyzed, where α-D-glucose was considered as the standard ligand for validating the Autodock 4.2 results. The binding energy of these compounds with interacting residues including H-bond interacting residues and Van der Waals interacting residues, along with the number of H-bonds are listed in Table 6. The simulation results of Autodock 4.2 simulation are shown in Fig. 15B, and the α-glucosidase-daidzein inhibitor complex showed a -7.16 kcal/mol binding energy for four hydrogen bonds. The nitrogen group of HIS295 residue was involved with hydrogen bonding interaction with an oxygen (O1) of daidzein with bond distance 3.12 Å. The oxygen group of ALA292 and nitrogen group of HIS295 were involved with strong hydrogen bonding interaction with O2 of daidzein having bond distance 3.08 and 3.13 Å, respectively. Oxygen group of ARG270 was involved with hydrogen bonding interaction with O4 of daidzein having bond distance 2.73 Å. In addition, hydrophobic interactions were also observed between ASN259, ILE262, ARG263, VAL266, ILE272, SER292, GLU296, LEU297, and SER298 residues. All of these hydrophobic interactions are important to strengthening the protein-ligand interaction and for positioning of daidzein in the catalytic pocket in order to inhibit the activity of α-glucosidase. On the other hand, genistein binding affinity with α-glucosidase was a -7.42

kcal/mol for five hydrogen bond. The nitrogen group of LYS16 residue was involved in strong hydrogen bonding interaction with an oxygen (O4) of genistein with bond distance 2.73 Å. The oxygen groups of THR290, and ASP341 residues were involved in strong hydrogen bonding interaction with O2 of genistein with bond distance 2.86 and 2.95 Å, respectively. The oxygen groups of ASN259 and GLU296 residues were involved with a strong hydrogen bond with O5 of genistein with bond distance 3.16 and 2.94 Å, respectively. In addition, some hydrophobic interactions were involved with the TRP343, ALA292, CYS342, LEU297, SER298, THR274, TRP15, ILE272, and LYS13 interacting residues. These interactions may provide further stability to the genistein-α-glucosidase complex and may help genistein fit well in the active site pocket of α-glucosidase (Fig. 15C). In addition, the α-glucosidase-calycosin inhibitor complex showed a -7.31 kcal/mol binding energy for five hydrogen bonds with interacting residues ARG270, SER291, ALA292 and HIS295. The oxygen groups of SER291 and ALA292 were involved in hydrogen binding interaction with oxygen (O5) of hydroxyl group of calycosin with bond distance 2.56 and 2.99 Å. Two nitrogen groups of HIS295 residue were involved in hydrogen binding interaction with oxygen (O1 and O5) of calycosin with bond distance 2.91 and 3.03 Å. Moreover, the oxygen group of ARG270 residue was also involved in strong hydrogen binding interaction with O4 of calycosin with bond distance 2.49 Å. In addition, hydrophobic interactions were also observed between the ASN259, ILE262,

ARG263, VAL266, GLU271, ILE272, GLU296, LEU297, and SER298 residues (Fig. 15D). As shown in Fig. 14, the docking results revealed that the binding sites on α-glucosidase for compounds were not the same as the binding site for α-D-glucose, a known competitive inhibitor, and these tested compounds formed more hydrophobic interactions with α-glucosidase than did α-D-glucose. In addition, both daidzein and calycosin interacted with the ARG270, ALA292, and HIS295 residues by forming a hydrogen bond and with the ASN259, ILE262, ARG263, VAL266, ILE272, GLU296, LEU297, and SER298 residues by hydrophobic interactions. Moreover, the molecular docking results of α-glucosidase are in close agreement with the experimental data with respect to the inhibition activities caused by active compounds.

Table 6. Molecular interaction results of the α-glucosidase active sites with the known inhibitor (α-D-glucose), daidzein, genistein and calycosin

Compound	Binding energy [a] (kcal/mol)	No. of H-bonds	H-bond interacting residues [b]	Van der Waals bond interacting residues [c]
α-D-Glucose	-6.74	10	GLU277,ARG442, ASP352, ASP69, HIS351, ARG213	TYR72, ASP215, PHE159, PHE178, VAL216, HIS112
Daidzein	-7.16	4	ARG270,ALA292, HIS295	ASN259,ILE262,ARG263, VAL266,ILE272,SER292, GLU296,LEU297,SER298
Genistein	-7.42	5	LYS16, THR290, ASP341, ASN259, GLU296	TRP343,ALA292,CYS342 ,LEU297, SER298, THR274, TRP15, ILE272, LYS13
Calycosin	-7.31	5	ARG270,SER291, ALA292, HIS295	ASN259,ILE262,ARG26, VAL266,GLU271,ILE27, GLU296,LEU297,SER298

[a] The semi-empirical free-energy force field was used to predict the binding free energies of protein-ligand complexes of a known structure and the binding energies of both the bound and unbound states. [b, c] All amino acid residues were located 3.75 Å from the original enzyme/inhibitor complex in the Autodock 4.2 program.

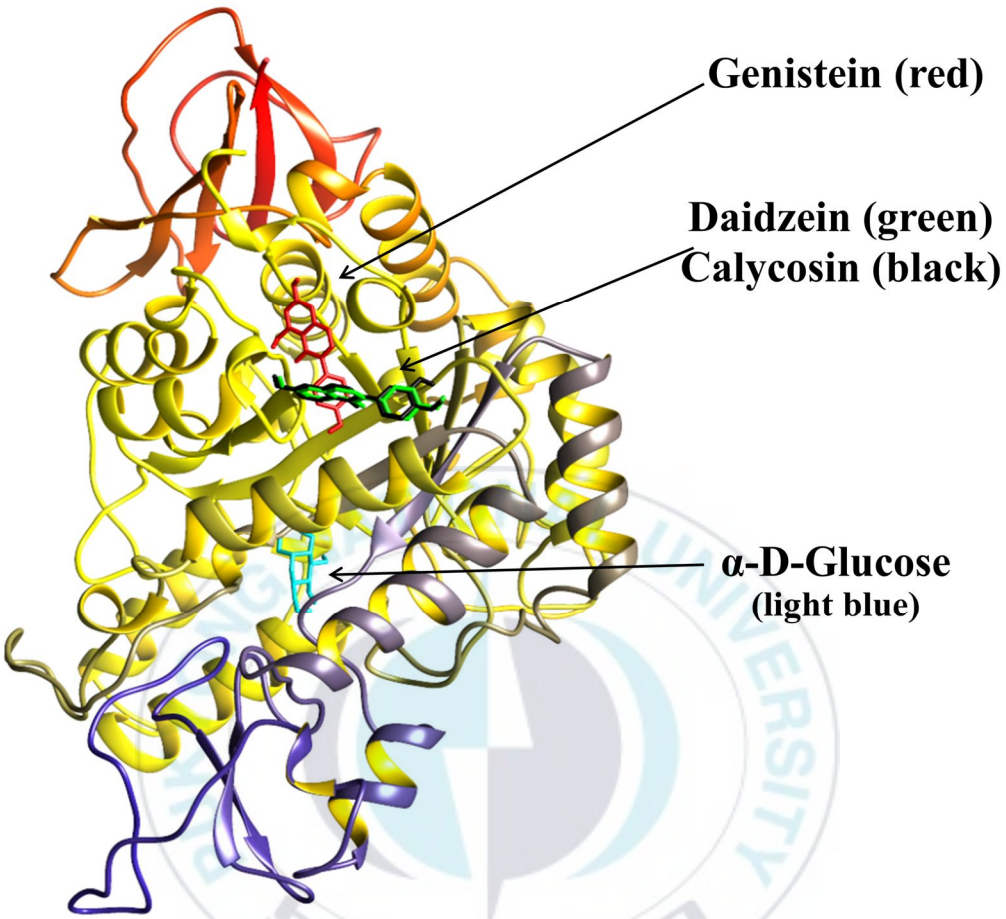

Fig. 14. Molecular docking models of the α-glucosidase inhibition of α-D-glucose daidzein, genistein, and calycosin.

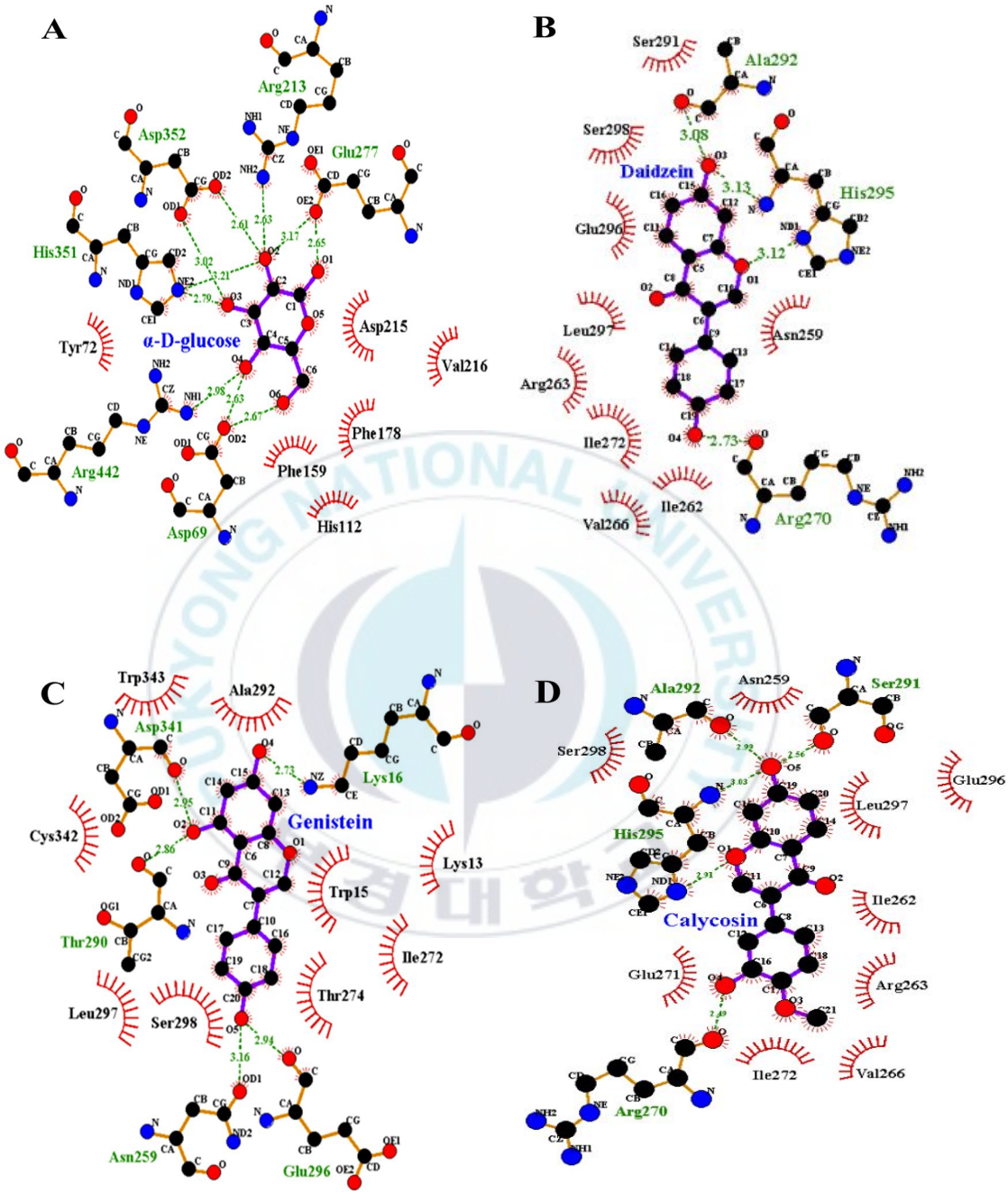

Fig. 15. Ligand interaction diagram of α-glucosidase inhibition of (A) α-D-glucose, (B) daidzein, (C) genistein, and (D) calycosin.

IV. Discussion and conclusion

Protein tyrosine phosphatase 1B (PTP1B) is a negative regulator of the insulin signaling pathway, α-glucosidase increases the absorption of carbohydrates into the bloodstream. Therefore, identification of new PTP1B and α-glucosidase inhibitors with higher target selectivity is important to prevent diabetes mellitus. Research into the structure-activity relationship and mechanistic, pharmacological and synthetic studies to determine the selectivity of the enzyme inhibitors are needed (Chen et al, 2015). The root of *P. lobata* is widely used as health food and traditional medicine for treatment of diabetes mellitus and fever, and it is used as a major natural source of isoflavones containing puerarin, daidzein and genistein that have preventive activities against diabetes mellitus (DM), inflammation, and oxidation. In this study, we noted that the root of *P. lobata* was traditionally used to treat thirst-waste regarded as DM and tried to demonstrate why the root of *P. lobata* was included in the composition of Ok-cheon-san which is prescribed for thirst-waste in traditional Chinese medicine, via screening anti-diabetic effect including PTP1B and the α-glucosidase inhibitory activities of the root of *P. lobata* (Yoo et al, 2005). The 70% EtOH extract of *P. lobata* roots showed PTP1B and α-glucosidase inhibitory activity in dose-dependent manner. Among the five

solvent-soluble fractions of the 70% EtOH extract, the *n*-hexane and EtOAc fractions showed potent PTT1B inhibitory activities, while the CH_2Cl_2 fraction showed potent α-glucosidase inhibitory activity compared to the other fractions. Moreover, we isolated active compounds toward inhibition of PTP1B and α-glucosidase from the root of *P. lobata*, especially lupane-type triterpenoids such as lupeol and lupenone that showed significantly potent PTP1B inhibitory activity, as well as isoflavones such as puerarin, puerarol and daidzein, which also showed potent PTP1B inhibitory activity. In prior studies, Li et al. (2014) and Na et al. (2009) reported that lupeol has better PTP1B inhibitory activity than lupenone. However, our results showed that lupenone (15.11 ± 1.23 μM) has a lower IC_{50} value with high PTP1B inhibitory activity compare to lupeol (38.89 ± 0.17 μM). The reason behind the higher activity of lupenone compare to lupeol was explained through enzyme kinetics and the molecular docking simulation study. A kinetic study using Lineweaver-Burk and Dixon plots demonstrated that lupeol and lupenone had noncompetitive-type inhibition against PTP1B to reduce the $0V_{max}$ values without changing the K_m values with respective K_i values of 13.88 μM and 21.24 μM. For the prediction of binding sites and energy after an *in vitro* assay of PTP1B, *in silico* docking studies can provide immense information about the orientation, strength and stability of ligand-protein interactions, and the program Autodock can plays an important role exhibiting the results. Computational docking studies provided important information for understanding

the mechanism behind active site binding interactions (Mane et al., 2011, Pawar et al., 2010). The catalytic activity of an enzyme molecule can be determined based on the hydrogen bonds identified in a docking study (Robert, 1998). The active site of PTP1B is defined by residues 214–221 belonging to the P-loop, which contains the catalytic CYS215 residue and binds the phosphate group. The WPD loop, which contains the ASP181 residue contributes considerably to the recognition of the peptide substrate. The inhibitor/substrate is readily accessible to the PTP1B binding pocket in the open-form of the WPD-loop. After inhibitor/substrate binding, active sites are blocked by the WPD-loop. The CYS215 residue then dephosphorylates the phosphocenter of the substrate through the nucleophilic attact. TYR46 and PHE182 residues indicate the depth of the protein tyrosine-binding pocket. Other important residues including ARP47, LYS120, and VAL49 residues demonstrates electrostatic, hydrophobic interactions, and hydrogen-bonding interaction. Since many of the amino acid residues around the active sites are considerably conserved in PTPs, an investigation of peripheral binding sites or secondary binding pocket sites located in the other sites with the conserved active site is required to design selective PTP1B inhibitors (Lee et al., 2007; Choi et al., 2015). By observing the chemical structure of lupenone and lupeol, it is clear that ketone and hydroxyl groups are present, respectively (Fig. 13). The oxygen atom of the ketone group in the lupenone structure is involved with two hydrogen bonds with PTP1B active site

residues CYS215 and ALA217 showing a -8.53 kcal/mol binding energy. Compound 23, a reported inhibitor of PTP1B forms 11 hydrogen bonds with active site residues of PTP1B including SER216, ARG221, ALA217, ILE219, GLY220, ARG254 and ASP48 residues (Table 5 and Fig. 13A). It is noticeable that both compound 23 and lupenone interact with the ALA217 active site residue of PTP1B by forming a hydrogen bond. In addition, the SER205 residue interacted with the oxygen atom of the hydroxyl group of the lupeol structure by forming a hydrogen bond having 2.81 Å bond distance. In contrast to the lupeol binding energy (-8.03 kcal/mol), lupenone showed lower binding energy with higher binding affinity. In addition to the hydrogen bonding interaction, other hydrophobic interactions helped produce the higher binding affinity of lupenone toward PTP1B. Although lupenone showed higher inhibitory activity, lupeol was also showed good inhibitory activity against PTP1B. The results of *in silico* molecular docking simulation study are correspond with the results of *in vitro* PTP1B inhibitory assay which showed lupenone has more high PTP1B inhibitory activity than lupeol. According to the results, lupenone containing a ketone group involved with two hydrogen bonds where lupeol containing hydroxyl group involved with one hydrogen bond and lupenone had more low IC_{50} value than lupeol. Thus, lupane-type triterpenoids with a ketone group are more effective for inhibiting PTP1B than are those with a hydroxyl group (Fig. 12).

Considering the α-glucosidase inhibitory potential, strong α-glucosidase inhibitory activities were observed at daidzein, genistein and calycosin belonging to isoflavone. Moreover, tuberosin, puerarol, lupenone, and lupeol also revealed potent α-glucosidase inhibitory effect. In a prior study, Choi et al. (2010) and Liu et al. (2015) reported that daidzein and genistein showed potent inhibition on α-glucosidase. However, the potency of calycosin isolated from *P. lobata* was first reported in this study, and we tried to determine the mechanism of action and the structure-activity relationship between α-glucosidase and isoflavones using enzyme kinetics and molecular docking simulation. The kinetic study demonstrated that active compounds, daidzein, genistein and calycosin showed noncompetitive-type inhibition against α-glucosidase with respective K_i values of 17.64μM, 5.03μM and 13.83μM. The prediction of binding sites and energy after the *in vitro* assay of α-glucosidase using molecular docking studies also showed that the binding sites between α-glucosidase and active compounds were not the same as the binding site for α-D-glucose, a known competitive inhibitor (Fig. 14). α-D-Glucose interacted with ASP215, GLU277, and ASP 352 residues, which are conserved active site residues (Fig. 15A). The conserved ASP215 residue acts as the catalytic nucleophile, and the GLU277 residue acts as the general acid-base catalysis. Moreover, the role of the ASP352 residue is to stabilize the substrate in the course of catalysis to help boost the acid-base hydrolysis reaction (Yamamoto et al., 2010). In the results of the molecular docking study, daidzein, genistein and

calycosin has lower binding energy (-7.47 kcal/mol, -7.42 kcal/mol and -7.33 kcal/mol) with higher binding affinity compared to a standard ligand α-D-glucose (-6.74 kcal/mol) because these compounds formed more hydrophobic interactions with α-glucosidase than did α-D-glucose. In addition, both daidzein and calycosin interacted with similar residues by forming hydrogen bond and hydrophobic interactions. It is notable that daidzein and calycosin have similar binding sites and reveal effective α-glucosidase inhibitory activities.

In conclusion, our results confirmed that *P. lobata* roots and its constituents possess anti-diabetic activities including PTP1B and α-glucosidase inhibitory activities. Among the isolated compounds, lupane-type triterpenoid, lupenone and lupeol showed significantly high PTP1B inhibitory activities. Whereas, outstanding α-glucosidase inhibitory activity was exhibited via daidzein, genistein and calycosin. In addition, enzyme kinetics that scrutinized the type of enzyme inhibition and molecular docking simulation between the enzymes and active compounds supported the above results. Hence, a computational study and experimental validation may help to reveal new natural drug candidates against diabetes, providing intense rationale for the application of active compounds as drug candidates for the treatment of diabetes.

V. References

Berman, H. M., Battistuz, T., Bhat, T. N., Bluhm, W. F., Bourne, P. E., Burkhardt, K., Feng, Z., Gilliland, G. L., Iype, L., Jain, S., Fagan, P., Marvin, J., Padilla, D., Ravichandran, V., Schneider, B., Thanki, N., Weissig, H., Westbrook, J. D., and Zardecki, C. (2002). The protein data bank. *Acta. Cryst.* 58, 899-907.

Bernstein, F. C., Koetzle, T. F., Williams, G. J., Meyer, E. F. Jr., Brice, M. D., Rodgers, J. R., Kennard, O., Shimanouchi, T., and Tasumi, M. (1977). The protein data bank: a computerbased archival file for macromolecular structures. *J. Mol. Biol.* 112, 535–542.

Chen, P. J., Cai, S. P., Huang, C., Meng, X. M., and Li, J. (2015). Protein tyrosine phosphatase 1B (PTP1B): A key regulator and therapeutic target in liver diseases. *Toxicology* 337, 10-20.

Cho, N. J., and Yun, Y. J. (2003). Studies on application of *Radix Puerariae* main blended prescription from Donguibogam. *Korean J. Oriental Med.* 11, 19-36.

Choi, C. W., Choi, Y. H., Cha, M. R., Yoo, D. S., Kim, Y. S., Yon, G. H., Hong, K. S., Kim, Y. H., and Ryu, S. Y. (2010). Yeast α-glucosidase inhibition by isoflavones from plants of Leguminosae as an *in vitro* alternative to acarbose.

Journal of agricultural and food chemistry, 58, 9988-9993.

Choi, J. S., Ali, M. Y., Jung, H. A., Oh, S. H., Choi, R. J., and Kim, E. J. (2015). Protein tyrosine phosphatase 1B inhibitory activity of alkaloids from Rhizoma Coptidis and their molecular docking studies. *J. Ethnopharmacol.* 171, 28-36.

Cornish-Bowden, A. (1974). A simple graphical method for determining the inhibition constants of mixed, uncompetitive and non-competitive inhibitors. *Biochem. J*. 137, 143–144.

Cui, L., Na, M., Oh, H., Bae, E. Y., Jeong, D. G., Ryu, S. E., Kim, S., Kim, B. Y., Oh, W. K., and Ahn, J. S. (2006). Protein tyrosine phosphatase 1B inhibitors from *Morus* root bark. *Bio org. Med. Chem. Lett.* 16, 1426–1429.

Dixon, M. (1953). The determination of enzyme inhibitor constants. *Biochem. J.* 55, 170–171.

Goldstein, B. J. (2002). Protein-tyrosine phosphatases: emerging targets for therapeutic intervention in type 2 diabetes and related states of insulin resistance. *J. Clin. Endocrinol. Metab.* 87, 2474-2480.

González-Rodríguez, Á., Gutierrez, J. A. M., Sanz-González, S., Ros, M., Burks, D. J., and Valverde, Á. M. (2010). Inhibition of PTP1B restores IRS1-mediated hepatic insulin signaling in IRS2-deficient mice. *Diabetes* 59, 588-599.

Guariguata, L., Whiting, D. R., Hambleton, I., Beagley, J., Linnenkamp, U., and Shaw, J. E. (2014). Global estimates of diabetes prevalence for 2013 and projections for 2035. *Diabetes Res. Clin. Pract.* 103(2), 137-149.

Jin, S. E., Son, Y. K., Min, B. S., Jung, H. A., and Choi, J. S. (2012). Anti-inflammatory and antioxidant activities of constituents isolated from *Pueraria lobata* roots. *Arch. Pharm. Res.* 35, 823-837.

Kim, J. M., Lee, Y. M., Lee, G. Y., Jang, D. S., Bae, K. H., and Kim, J. S. (2006). Constituents of the roots of *Pueraria lobata* inhibit formation of advanced glycation end products (AGEs). *Arch. Pharm. Res.* 29, 821-825 .

Lee, S., and Wang, Q. (2007). Recent development of small molecular specific inhibitor of protein tyrosine phosphatase 1B. *Med. Res. Rev.* 27, 553–573.

Li, J. L., Li, N., Zhang, N., Ma, K., XING, S. S., and Cui, L. (2014). Lupane-Terpenoids isolated from *Betula platyphylla* Suk of protein tyrosine phosphatase 1B inhibitory activity. *Nat. Prod. Res. Dev.* 26, 1398-1401.

Li, T., Zhang, X. D., Song, Y. W. and Liu, J. W. (2005). A microplate-based screening method for alpha-glucosidase inhibitors. *Chin. J. Clin. Pharmacol. Ther.* 10, 1128-1134.

Lineweaver, H., and Burk, D. (1934). The determination of enzyme dissociation constants. *J. Am. Chem. Soc*. 56, 658–666.

Liu, B., Kongstad, K. T., Qinglei, S., Nyberg, N. T., Jäger, A. K., and Staerk, D. (2015). Dual high-resolution α-glucosidase and radical scavenging profiling combined with HPLC-HRMS-SPE-NMR for identification of minor and major constituents directly from the crude extract of *Pueraria lobata*. *J Nat Prod.* 78, 294-300.

Liu, Z. Q., Liu, T., Chen, C., Li, M. Y., Wang, Z. Y., Chen, R. S., Wei, G. X., Wang, X. Y., and Luo, D. Q. (2015). Fumosorinone, a novel PTP1B inhibitor, activates insulin signaling in insulin-resistance HepG2 cells and shows anti-diabetic effect in diabetic KKAy mice. *Tox. Ap. Pharm.* 285, 61–70 .

Lordan, S., Smyth, T. J., Soler-Vila, A., Stanton, C., and Ross, R. P. (2013). The α-amylase and α-glucosidase inhibitory effects of Irish seaweed extracts. *Food Chem.* 141, 2170-2176.

Ma, Y. M., Tao, R. Y., Liu, Q., Li, J., Tian, J. Y., Zhang, X. L., Xiao, Z. Y., and Ye, F. (2011). PTP1B inhibitor improves both insulin resistance and lipid abnormalities *in vivo* and *in vitro*. *Mol. Cell. Biochem*. 357, 65-72 .

Mane, R.S., Ghosh, S., Chopade, B.A., Reiser, O., and Dhavale, D.D. (2011). Synthesis of an adenine nucleoside containing the (8'R) epimeric carbohydrate core of amipurimycin and its biological study. *J. Org. Chem*. 76, 2892-2895.

Mun, S. C., and Mun, G. S. (2015). Dynamics of phytoestrogen, isoflavonoids,

and its isolation from stems of *Pueraria lobata* (Willd.) Ohwi growing in Democratic People's Republic of Korea. *J. Food and Drug analysis* 23, 538-544.

Na, M., Kim, B. Y., Osada, H., and Ahn, J. S. (2009). Inhibition of protein tyrosine phosphatase 1B by lupeol and lupenone isolated from *Sorbus commixta*. *J. Enzyme Inhib. Med. Chem.* 24, 1056-1059.

Parthasarathy, R., Ilavarasan, R., and Karrunakaran, C. M. (2009). Antidiabetic activity of *Thespesia Populnea* bark and leaf extract against streptozotocin induced diabetic rats. *Int. J. Pharm. Tech* . 1(4), 1069-1072.

Patel, A. M., Anand, I. S., and Suva, M. A. (2014). Role of protein tyrosine phosphatase-1B inhibitors in type 2 diabetes mellitus. *J. Pharm. Sci. Tech*. 4, 2-6.

Pawar, V. U., Ghosh, S., Chopade, B. A., and Shinde, V. S. (2010). Design and synthesis of harzialactone analogues: promising anticancer agents. *Bioorg. Med. Chem. Lett*. 20, 7243-7245.

Pettersen, E. F., Goddard, T. D., Huang, C. C., Couch, G. S., Greenblatt, D. M., Meng, E. C., and Ferrin, T. E. (2004). UCSF Chimera--a visualization system for exploratory research and analysis. *J. Comput. Chem.* 25, 1605-1612.

Prasain, J. K., Jones, K., Kirk, M., Wilson, L., Smith-Johnson, M., Weaver, C.,

and Barnes, S. (2003). Profiling and quantification of isoflavonoids in kudzu dietary supplements by high-performance liquid chromatography and electrospray ionization tandem mass spectrometry. *J. Agric. Food Chem.* 51, 4213-4218.

Qin, Z., Pandey, N. R., Zhou, X., Stewart, C. A., Hari, A., Huang, H., Stewart, A. F., Brunel, J. M., and Chen, H. H. (2015). Functional properties of Claramine: a novel PTP1B inhibitor and insulin-mimetic compound. *Biochem. Biophys. Res. Commun.* 458, 21-27.

Robert, H. C. (1998). A new type of hydrogen bond. *J. Sci*. 282, 2000-2001.

Szczepankiewicz, B. G., Liu, G., Hajduk, P. J., Abad-Zapatero, C., Pei, Z., Xin, Z., Lubben, T., Trevillyan, J. M., Stashko, M. A., Ballaron, S. J., Liang, H., Huang, F., Hutchins, C. W., Fesik, S. W., and Jirousek, M. R. (2003). Discovery of a potent, selective protein tyrosine phosphatase 1B inhibitor using a linked-fragment strategy. *J. Am. Chem. Soc*. 125, 4087-4096.

Wong, K. H., Li, G. Q., Li, K. M., Razmovski-Naumovski, V., and Chan, K. (2011). Kudzu root: traditional uses and potential medicinal benefits in diabetes and cardiovascular diseases. *J. Ethnopharmacol*. 134, 584-607.

Wu, K., Liang, T., Duan, X., Xu, L., Zhang, K., and Li, R. (2013). Anti-diabetic effects of puerarin, isolated from *Pueraria lobata* (Willd.), on streptozotocin-

diabetogenic mice through promoting insulin expression and ameliorating metabolic function. *Food Chem. Toxicol*. 60, 341-347.

Yan, J. K., Zhang, G. W., Pan, J. H., and Wang, Y. J. (2014). Alpha-Glucosidase inhibition by luteolin: Kinetics, interaction and molecular docking. *J. Biol. Macromol.* 64, 213– 223.

Yamamoto, K., Miyake, H., Kusunoki, M., and Osaki, S. (2010). Crystal structures of isomaltase from *Saccharomyces cerevisiae* and in complex with its competitive inhibitor maltose. *FEBS J.* 277, 4205-4214.

Yoo, J. L., Jang, D. S., and Kim, J. S. (2005). Quality evaluation of herbal prescription, Oc Chun San, employing simultaneous determination of the marker compounds by HPLC. . *Korean J. Oriental Med.* 11, 167-178.

Zhou, Y. X,, Zhang, H., and Peng, C. (2014). Puerarin: a review of pharmacological effects. *Phytother. Res.* 28, 961-975.